Universitat Politècnica de Catalunya
The University of Warwick

Bachelor's thesis in Engineering Physics

Mass and eccentricity constraints on the planetary debris orbiting the white dwarf WD 1145+017

POL GURRI

Supervisors:
Dr. Boris T. Gänsicke
Dr. Enrique García-Berro

June 2016

Abstract

An important fraction of planets are thought to continue orbiting their host stars even after their giant branch evolution. This prediction is endorsed by metal-polluted atmospheres of white dwarfs; disrupting planetary bodies can create a circumstellar debris disk from which the white dwarf may accrete metals. Although tidal disruption of planetesimals near the Roche limit has been long theorised as a polluting mechanism, visual confirmation of this process was not supplied until the recent discovery of several bodies transiting the white dwarf WD 1145+017.

To date, not much is known about the exact origin and nature of the orbiting bodies nor about the process of disruption and posterior circularisation that lead to a dusty circumstellar debris disk. WD 1145+017 constitutes a complex system of many (at least 6) disintegrating bodies directly measurable from photometric transit light curves. On-going observations are providing transits with precision on the order of seconds, and phase shifts between the bodies. However, the multiplicity, size, mass and eccentricity of the debris are among the still unknown properties, some of them unconstrained within many orders of magnitude.

In this work we provide a computational study for the system WD 1145+017 by using N-body simulations. Using a modified version of the MERCURY code it has been possible to track the behaviour of planetesimals orbiting a white dwarf for time-spans up to five years. Furthermore, from analysing the many-body interactions it was possible to obtain period deviations from the observed orbits and determine for which arrangements there are greater chances of long-term dynamical stability. As a result, this work gives new insight on the WD 1145+017 system and sets more strict boundaries for the mass and eccentricity of the orbiting bodies. A direct comparison is also made between phase shifts provided by observations and our simulations.

Acknowledgments

I would like to express my deep gratitude to Dr. Boris T. Gänsicke for allowing me to become part of his research team with little prior knowledge of my experience. His continuous and enthusiastic encouragement during the whole project have been very much appreciated. Furthermore, I would like to thank him for offering me the chance to participate in future projects related to this work. I would also like to express my very great appreciation to Dr. Enrique García-Berro for all his advice, both in a professional and personal sense, which went well beyond his duties. I cannot imagine any of these experiences without him. My grateful thanks are also extended to Dr. Dimitri Veras for his valuable and constructive suggestions during my stay. His willingness to help together with his fast and detailed answers have been essential for me. I also want to thank him for all the personal advice he has given to me. I also want to acknowledge the Engineering Physics staff and professors for such a devoted task. Thanks to their daily and often not mentioned efforts many of us will have a brighter future.

I am extremely thankful for all the friendships I created with the people from The University of Warwick, they have made this experience incredible. Their willingness to help and share good moments together made me feel like home. I also want to thank all my friends from UPC for walking together with me during this 4 last years. The friendships made there will certainly be life-lasting. Finally, I am immensely thankful for the love received from all my family, for being there during good and bad times, and for their never-ending trust in me.

Contents

1

Motivation

Beyond the sky, far from our Earth, lies the vast expanse of the Universe. The deeper we see into space, the more we discover. There are countless galaxies, each hosting hundreds of billions of stars being orbited by planets and asteroids. We find out about the Universe through light, which may have been reflected, absorbed and re-emitted, but its origin can often be found in the very heart of the stars. Some of those celestial bodies are so far away that the light arriving today to Earth left them millions of years ago, opening to us a unique window to the past.

Sunken in a sea of stars, mankind has long speculated about the possibility of life existing on distant planets. Throughout history we have been trying to observe and understand what lies beyond the ultimate frontier, but only recently have we been able to detect planetary systems similar to ours. As these systems are billions of times fainter than their host stars, detecting planets requires an extraordinarily demanding study of light.

Another great discussion topic has always been the fate of the Earth. Little is known about how planets can survive the inevitable transformations their host stars undergo. In about 5 billion years, the sun's hydrogen fuel supply will run out and, after increasing in size and probably swallowing some planets, it will expel its outer layers and become what it is known as a white dwarf.

Although a significant fraction of planets are thought to survive such process, only one system has been observed to subsist after the transformation of its star into a white dwarf. Being the first of its kind, WD 1145+071 provides a new avenue to understand the interactions between planets and the final evolutionary state of most of the stars, the white dwarfs.

2

White dwarfs

2.1 | General background

White dwarfs are the final evolutionary state of all stars that do not have enough mass to form a neutron star or a black hole. This matter translates into about 95% of all the stars in the Universe (97% in the Milky Way) becoming white dwarfs at some point in their lives. These types of star exhibit volumes comparable to that of the Earth but with extremely larger masses, more comparable to the Sun's. Nevertheless, white dwarf stars are not broadly studied only because most stars, including our Sun, will become one, but also because they are very old objects and therefore carry valuable information about the history of the Universe.

Almost everything we know about the Universe is thanks to a cautious study of light that traveled through space towards the Earth. Light often is the result of nuclear fusion processes in the cores of the stars. Gravity pulls the star toward its center, increasing its pressure and temperature to extreme values that warrant nuclear fusion's requirements. When nuclear fusion takes place, energy is released and the center pushes back strongly enough to prevent gravity from further compressing the star. The extra energy liberated by nuclear fusion is emitted in the form of light. As long as a star has plenty of fuel, fusion will continue, and the star will be stable and shining.

White dwarf stars are formed when a star runs out of fuel, gravity takes over again and the star rapidly collapses. During the compression, matter gets extremely squashed and electrons, repelling each other, create resistance against further confining. Thus, the electron pressure created due to gravity prevents the star from totally collapsing. White dwarfs shine simply from the release of left-over heat from when the star was still undergoing nuclear reactions. As time passes, they radiate all their remaining energy and gently cool down. A white dwarf's cooling time can be longer than the age of the Universe and therefore, the coldest white dwarfs stars are among the oldest objects in the Universe.

White dwarf's surfaces are directly observable using traditional methods (like spectroscopy or stellar atmosphere modeling via transits), which makes white dwarfs easier to study than other old, high-dense objects like neutron stars or black holes. Employing these highly used techniques, it has been possible to provide reliable data for effective temperatures, surface gravities, chemical abundances, masses, radii and even ages of such stars. Furthermore, white dwarfs offer the possibility of studying matter under very extreme conditions, at temperatures and densities that are impossible to achieve on Earth. In this way, white dwarfs contribute to other fields of current research, like quantum physics, supplying data about electron degeneracy and neutrinos among others.

Once recognized the relevance of such objects, this chapter provides some general background about white dwarfs. This includes a brief historical timeline and reviews about how they are formed, their main properties, classification, internal composition and the energy sources they rely on.

Further reading about white dwarfs.[1–3]

2.2 | History

The beginning of the 20th century was one of the brightest moments in the history of science. That epoch gave birth to the first quantum theory (1900), the wave-particle duality (1905), the special (1905) and general (1915) theories of relativity, the discovery of atoms (1911)... It was also back then (1910) when Henry Norris Russell, Edward Charles Pickering and Williamina Fleming, discovered that despite being a really faint star (same luminosity as an M dwarf), 40 Eridani B was a white star (spectral type A). This finding, being an exception on star spectral analysis, later established the name "white dwarf".

The stellar remnant 40 Erdiani B, later studied by Russell (1914)[4] and Walter Adams (1914)[5] (who provided a detailed spectral study of the star), revealed the existence of a very different star nature, white dwarfs. Nevertheless, it was Sirius B that showed the first properties of a white dwarf. The mass of Sirius B was known to be near $1 M_\odot$, thanks to the interaction with its companion Sirius, but it did exhibit a hotter surface temperature and much lower luminosity than all the known hot typical (main sequence) stars.

Knowing the distance to Sirius and the surface temperature of Sirius B (via spectral and luminosity studies), Walter Adams (1915)[6] found the value of its radius and therefore the internal density of that peculiar star. The resulting density was $\rho \sim 10^4\,\mathrm{g\,cm^{-3}}$ (nowadays a value of $\rho \sim 10^6\,\mathrm{g\,cm^{-3}}$ is accepted), which was a completely bizarre density at that time. Adams (1925)[7] provided an independent measure of the density by determining the gravitational redshift created by Sirius B, which led to a similar result. This discovery led Arthur Stanley Eddington (1928)[8] to state that *"Professor Adams...has confirmed our suspicion that matter 2,000 times denser than platinum is not only possible, but is actually present in the Universe"*.

An explanation for this tremendous density remained a mystery until Ralph H. Fowler (1926)[9] provided a plausible explanation using quantum mechanics and Fermi-Dirac (1926)[10] statistics. Fowler presented that a gas of almost fully degenerate electrons is capable of creating enough pressure to support the star and prevent it from gravitational collapse. The density of the theoretical degenerate electron gas was as enormous as the estimate for Sirius B.

After Fowler's work, many renowned astrophysicists like Wilhelm Anderson (1929),[11] Edmun Stoner (1930),[12] Subrahmanyan Chandrasekhar (1931)[13] and (1939)[14] or Donald D. Clayton (1968)[15] among others, contributed to the research on white dwarfs. Thanks to their works it has been possible to determine that white dwarfs can be modelled as a zero temperature gas made of degenerate electrons following Fermi-Dirac statistics, and thus demonstrate that white dwarfs have a maximum mass, also known as the Chandrasekhar mass. This upper limit is generated due the maximum speed at which electrons can move, the speed of light. The concept of a maximum mass turned out to be of great importance in stellar evolution, and it has been shown to be a key factor in determining the end state of all stars in the Universe.

Nowadays there are numerous research groups devoted only to the study of white dwarfs, there are more than 20,000 confirmed white dwarfs and more than 100 papers about them were published during the last year 2015.

Further reading about white dwarf history.[16]

2.3 | Formation

Galaxies are mainly formed of stars, stellar remnants and the interstellar medium, which is made out of gas (mostly hydrogen and helium) and dust. Higher density regions of the interstellar medium form clouds, also known as nebulae, where star formation originates. Stars are born from the condensation of a gas; individual molecules, and then groups of them, undergo gravitational attraction on each other, gathering themselves closer together. If a cloud is massive enough that the gas pressure is insufficient to counter the effects of gravity (*i.e.* greater than the Jeans mass[17]), the cloud will undergo a gravitational collapse. This "protostellar" cloud will continue to contract and its density and temperature will increase until they are high enough to dissociate and ionize atoms. At this stage, the cloud rapidly compresses even more to reach temperatures suitable for hydrogen fusion, point at which a new star is formed.

The different stages of the stellar evolution can be observed in the Hertzsprung-Russell diagram (*Figure* 2.1), which is one of the most useful and powerful plots in astrophysics. It originated when Ejnar Hertzsprung (1911)[18] plotted the absolute magnitude of stars against their effective temperature. Later on, Henry Norris Russell (1913)[4] represented the spectral class against the absolute magnitude of stars. Their plots combined showed that the relationship between temperature and luminosity of a star is not random but instead appears to split in different groups or stages.

After a star has formed and it starts to burn hydrogen, it enters the main sequence band, where stars are dominated by hydrostatic equilibrium. The equilibrium occurs when external forces such as gravity are balanced by a pressure gradient force created by the energy released via fusion in the cores of stars. The temperature and density of the core are self-regulated to maintain the star stable. A sudden reduction in the core energy production will cause the star to collapse, increasing the temperature and density in the core, and consequently creating an increase of the energy production rate up to its initial state. The same reasoning can be applied in the opposite direction, increasing the rate of energy production forces the star to expand, which reduces its temperature and density in the core, and therefore, lowers again the fusion rate. Stars are therefore self-regulating systems during their main-sequence lifetime. The majority of stars can be found along the main-sequence stage, a line on the Hertzsprung-Russell diagram, in which both the spectral type and the luminosity depend only on the star's mass.

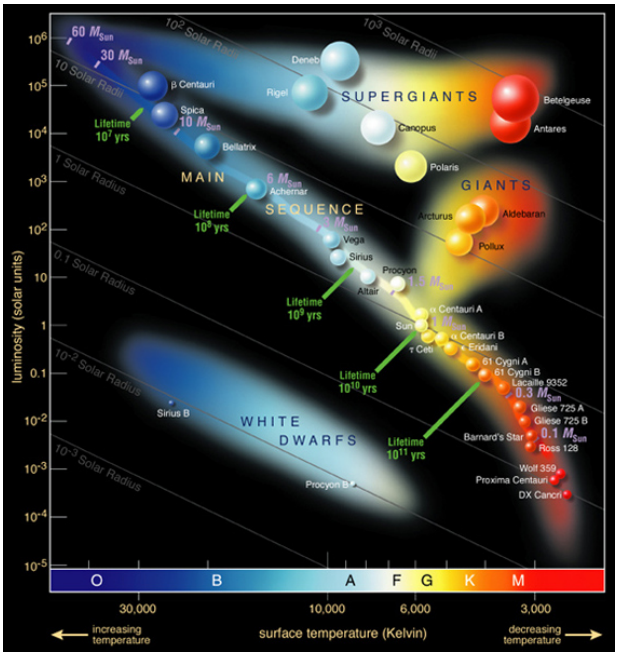

Figure 2.1: Hertzsprung-Russell diagram. The location of the white dwarf phase is located well below the main sequence stage. From ESO.

When a main-sequence star consumes most of its hydrogen, the loss of energy generation causes the star to contract due to gravitational collapse. Depending on the mass of the star it will follow different evolutionary paths. Low mass stars (less than $\sim 0.2M_{\odot}$) directly become white dwarfs. Stars with greatest masses start burning other elements and later expand and decrease in temperature entering the domain of red giants in the Hertzsprung-Russell diagram. During their life, all stars face a moment when they cannot continue fusing elements in their interiors. After a star is depleted of its fuel it will inevitably undergo gravitational collapse and its mass will determine its fate once more. If the mass of the star in the range of $\sim 0.07M_{\odot}$ to $\sim 10M_{\odot}$ the star will expel its outer layers and leave behind its core, the remnant white dwarf. On the other hand, more massive stars end their lives in the form of even more extremely dense objects like neutron stars (for stars with mass between $\sim 10M_{\odot}$ to $\sim 20M_{\odot}$) or black holes (for stars with mass greater than $\sim 20M_{\odot}$).

The matter inside a white dwarf cannot initiate fusion reactions, thus the star has no energy source. White dwarfs are supported solely by electron degeneracy pressure, resulting in a really dense star. The physics ruling the electron degeneracy specifies the Chandrasekhar limiting mass ($\sim 1.45M_{\odot}$), beyond which the star cannot be supported by electron degeneracy pressure and therefore a white dwarf cannot exist.

Because of their stellar nature, white dwarfs are very hot when formed, but since they have no energy source, they radiate all their internal energy and cool down. As time passes, white dwarfs reduce in temperature, and therefore also does their color, until they eventually become black dwarfs, which are faint, cold and very dense objects. The time it takes for a white dwarf to lose all its energy has been calculated to be longer that the current age of the Universe, and therefore, no black dwarfs can yet exist.[19,20]

Further reading about white dwarf formation.[1,2,15,19,21,22]

2.4 | Classification

More than 100 years of observational and theoretical studies of white dwarf have allowed us to determine that these slowly cooling star corpses are curiously homogeneous. Koester, Schulz and Weidemann (1979)[23] showed how the mass function for all white dwarfs is very narrow ($\sigma \sim 0.1$) and peaks at $\sim 0.55 M_{\odot}$. This finding demanded a new, non-mass-related way of classifying these stars. Sion *et al.* (1983)[24] proposed a new white dwarf classification system were white dwarfs are classified by atmospheric abundances revealed by spectroscopic observations (*e.g.* *Figure* 2.2).

There is a clear division in white dwarf spectral types. The most common nature is the hydrogen-rich atmosphere group (type DA using Sion *et al.* nomenclature), which includes almost 85% of the current population of white dwarfs. The remaining 15% are known as the non-hydrogen-rich white dwarfs (type non-DA), which are mostly composed of stars showing helium lines in their atmospheres (type DB).

DA white dwarfs are found over a very large range of effective temperatures, from 6,000K to more than 100,000K. It is important to notice that although the vast majority of their atmosphere is composed of hydrogen, there are also traces of other elements. The non-DA group stars are thought to lack hydrogen due late thermal flashes experienced by post-AGB progenitors.[25,26] This group is divided in different subgroups, the DO spectral type with effective temperatures ranging from 45,000K to 200,000K that show relatively strong lines of singly ionized He (He II), the DB type ranging from 11,000K to 30,000K, with strong neutral He (He I) lines, and the DC, DQ, and DZ types with effective temperatures smaller than 11,000K showing traces of carbon and metals in their spectra.

A more detailed spectral classification of the different kinds of white dwarfs can be found in *Table* 2.1. Note that the classification system can be combined, including therefore more than one kind (*e.g.* DAH, DABZ).

Spectral classification	Intrinsic characteristics
DA	H Balmer lines, no metals or He
DB	He I lines, no metals or H
DC	Continuum spectrum, no remarkable lines
DO	He II, small He I or H
DZ	Metal lines (other elements than H or He)
DQ	Carbon features present
P	Detected magnetic polarization
H	Detected Zeeman splitting
X	Non-classified
V	Detected variabilities

Table 2.1: White dwarf spectral classification

Furthermore, the ratio of DAs vs non-DAs greatly depends on the effective temperature of the star.[27] This finding lead Fontaine and Wesemael (1987)[28] to suggest that the dominant photospheric constituent of white dwarfs evolves with time, a process that is known as spectral evolution. Spectral evolution is usually caused due to convection, mass-loss, accretion or gravitational settling. A non-DA white dwarf can turn into a DA because of gravitational settling; heavier elements sink into the white dwarf and the outer layer is therefore formed mainly of hydrogen. DAs may turn into non-DA because of mass-loss or accretion for instance.

The chemical composition of a white dwarf is strongly related to the progenitor main-sequence star. The nuclear reactions that happened in the past are the responsible for the different atmospheric compositions the white dwarfs shows now. DAs for instance have 95% of their mass provided by a carbon-oxygen core, which is the result of the progenitor star burning helium into carbon through the triple-alpha process. As we move from the inside out of a DA white dwarf we can see how oxygen and carbon disappear leaving room for: (i) a layer of He (usually called He-buffer) formed due to previous H burning and (ii) an outer layer of H separated from the He via gravitational settling.

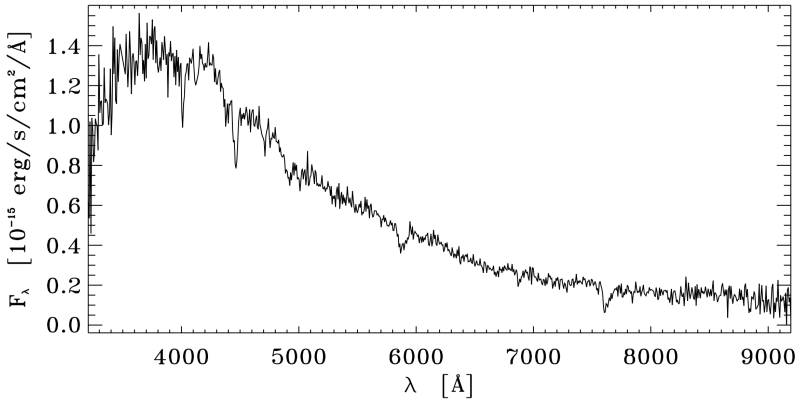

Figure 2.2: WD 1145+017 spectrum from the Hamburg/ESO survey from Friedrich *et al.* (2000).[29] Although far from a perfect example, WD 1145+017 presents a DBZ spectrum (the original spectrum did not show signs of metals and therefore the star was classified as DB).

Further reading about white dwarf classification.[1,2,24]

2.5 | Internal composition

White dwarf stars are extremely dense objects, resulting in high values of pressure and temperature in their cores. This high pressure and temperature are enough to ionize all the matter within the core and transform it into a degenerate electron gas.[9] The chemical potential of the electron gas is much greater than its thermal energy, which translates into a step-like function for the Fermi-Dirac distribution that characterizes electrons. Thus, all energy states with lower energy than the Fermi energy are occupied. It is possible then to approximate the electrons in the core as a completely degenerate electron gas at zero temperature. The Pauli exclusion principle implies that a pair of electrons (one for each spin orientation) cannot occupy the same state as another pair, even under the pressure of a collapsing star of several solar masses. In this way, electrons are forced to very high momentum states. When the spatial volume is decreased, these electrons provide the major part of the pressure which stabilizes the star against gravity. The electrons with energies close to the Fermi energy contribute the most to pressure.

Degenerate structures are almost perfect conductors and their pressure does not depend on the temperature but on the speed of the degenerate particles. Increasing speed rises the mass of the particles, which increases the gravitational force pulling the particles closer together. Therefore, in degenerate gas structures, when the pressure is increased the object becomes smaller, which leads to extremely large densities. Also, because inside perfect conductors electrons hardly collide among them, it is possible to treat

mechanical and thermal structures separately. For mechanical structures its is possible to apply a zero temperature gas approximation. Unluckily, thermal structures cannot be approximated in this way as the star radiates because of its internal temperature.

Chandrasekhar (1931)[13] developed the zero-temperature gas approximation for the mechanical structure of white dwarfs, assuming non-interacting and completely degenerate electrons. In the limit of complete degeneracy, the electron pressure can be considered only due the energy states below the Fermi energy. Using that fact and combining it with the equations of hydrostatic equilibrium and mass conservation, Chandrasekhar showed how the problem can be addressed as a second order differential equation with two free parameters: the central density and the molecular weight per electron.

$$\frac{\mathrm{d}}{\mathrm{d}r}\left(\frac{r^2}{\rho}\frac{\mathrm{d}P}{\mathrm{d}r}\right) = -4\pi G r^2 \rho \tag{2.1}$$

Where $\rho = Cx^3$, $x = p_f/m_e c$, $C = 8\pi m_e^3 c^3 \mu_e M/3h^3$, and μ_e the electron molecular weight. The other constants have their usual values.

For a fixed value of the electron molecular weight ($\mu_e \sim 2$ for carbon-oxygen composition) it is possible to integrate *Eq.* 2.1 for different values of the central density, which establishes a unique relation between mass and radius. This famous mass-radius relation also sets a limiting mass when the density tends to infinity and the radius approaches zero. This mass is known as the Chandrasekhar limiting mass ($\sim 1.45 M_\odot$ for carbon-oxygen white dwarfs). Larger masses would lead to non-stable white dwarfs as the gravity would be stronger than the degenerate electron pressure. This limiting mass is closely related with Type Ia (thermonuclear) supernovae, some of the most energetic events in the Universe.

Chandrasekhar's model provides a good description of the mechanical structure of a white dwarf. The equivalent model for the thermal structure was made by Mestel (1952)[30] assuming that the white dwarf is not actually at zero temperature. This model explains two concepts: how much energy does the white dwarf has, and how quickly it looses it. To address the first concept we can assume that all the core is at the same temperature, which is a good approximation for cold white dwarfs because degenerate electrons are very good at heat transportation. The second concept needs the use of heat transportation equations for the envelope, which is a fairly thin layer where temperature drops substantially. In the envelope it is not possible to assume electron degeneracy and therefore heat transfer is performed by less efficient mechanisms such as convection and/or radiation.

If it is assumed that the energy is transported by radiation (a good approximation for hot white dwarfs), putting together the equation of hydrostatic equilibrium with the radiative transport leads to *Eq.* 2.2.

$$\frac{\mathrm{d}T}{\mathrm{d}r} = -\frac{3}{4ac}\frac{\kappa\rho}{T^3}\frac{L_r}{4\pi r^2} \tag{2.2}$$

Where L_r is the luminosity through the sphere of radius r and κ is the radiative opacity.

Assuming that nuclear energy is not involved so that total luminosity is almost equal to L_r, that the pressure is due an ideal gas of ions and electrons and that the core is unithermal, it is possible to find a relation between the mass and the luminosity of the white dwarf. Those are large approximations which are not usually verified in white dwarfs,

but they give a general idea of the behavior of the envelope's heat transportation. Mestel (1952)[30] found that for a one solar mass white dwarf with a luminosity 10^{-4} times that of the Sun, its temperature is around 10^6 K, which provides a approximate idea about the relationship between temperature and luminosity of white dwarfs. With a deeper analysis of the equations it is possible to prove that white dwarfs undergo a cooling process where its core chemical composition determines its cooling speed. Moreover, the more massive a white dwarf is, the lower its radius, which implies less luminosity and therefore longer cooling times.

Further reading about white dwarf composition.[1–3, 14, 30]

2.6 | Energy sources

White dwarfs experience a cooling process that slowly lowers their temperature and therefore their internal energy. Although most of the energy loss is due to light radiation through the envelope there are other processes by which the star loses energy. This section gives an overview of the most significant ones.

Light radiation. As mentioned in the previous section, there is an energy leak through the thin, non-degenereate envelope. The light emitted by the star can be modeled using Mestel's (1952)[30] equation, which provides the luminosity of the star ($L = KMT^{7/2}$ where K depends on the opacity of the envelope). In this way, the hotter the star is, the more it radiates.

Nuclear energy. The role of nuclear burning as a main energy source ceases as soon as the hot white dwarf reaches the cooling branch and starts decreasing in temperature. However, nuclear processes never stop completely, and during the whole life of the star unstable nuclear burning may be relevant. This unstable nuclear burning happens in the exteriors shells of white dwarfs, where occasionally hydrogen (via the CNO cycle) and helium can be burned. The energy produced by these events is rapidly radiated away.

Gravitational energy. The radii of white dwarfs change over time. Gravitational forces shrink the white dwarf to as little as half the initial radius over its cooling age. This contraction is by no means negligible, and it can be the responsible for up to 30% of the star's luminosity. After the first hot stage of the white dwarf, its gravitational energy does not contribute to the luminosity but mainly to increase the Fermi energy of the degenerate electrons.

Neutrino losses. Within white dwarfs neutrinos are created from photons. Through a process called the plasmon neutrino process, a single photon in a plasma decays into a neutrino-antineutrino pair. Because neutrinos barely interact with matter, they have no opposition to leave star and result in a big energy leak, specially for hot white dwarfs. Neutrino losses can actually be precisely calculated thoughtout the hydrogen-exhausted cores of white dwarfs.[31]

There are also other mechanisms by which a white dwarf can lose energy. For example, crystallization of the carbon-oxygen core or gravitational settling of minor species in the core are two main energy-lose processes that need to be addressed with thermodynamics of high-dense matter.

Further reading about white dwarf energy sources.[1, 30–32]

3

Planets

3.1 | Planet formation history

To a first approximation, planets can be defined as large spherical bodies orbiting stars. The main difference between planets and stars is that planets are not massive enough to power nuclear fusion in their cores. For this reason, planets have a maximum mass of approximately 13 Jupiter masses ($\sim 2.5 \times 10^{28}$ kg). A lower mass limit is not well defined; only massive enough bodies capable of clearing their neighborhoods of other large bodies are considered planets. Smaller, planet-like objects that fail to accomplish the last definition are known as planetesimals or dwarf planets.

The theoretical study of planet formation has a long history, and numerous books and review articles have been written about the topic. Kant (1755)[33] and Laplace (1796)[34] were the first to put the origin of planets in a scientific framework and developed the most widely accepted model for planet formation, the nebular hypothesis. This chapter reviews the basic aspects about planet formation under the general assumption of the nebular hypothesis.

Descartes' (1644)[35] work proved a breakthrough in planet formation; he argued that planets, as well as stars, were formed from a system of vortices. His early picture had no explanation for vortices formation and did not consider their rotation direction. Three hundred years later, Weizsäcker (1944)[36] presented for the first time the idea of a turbulent disk rotating around a star. This disk was responsible for hosting the vortices that, through the accretion of small particles, formed the planets. He was also the first to theorise angular momentum transportation in the disk, which explains how mass flows into the star and momentum is gained by the outer particles.

Kuiper (1951)[37] suggested that giant planets could form from Jeans instability in a similar way to stars. Supporting the idea, Cameron (1969)[38] showed that, enhanced by the effects of vortices, the protoplanetary disk could break up into axisymmetric rings which could then form planets by Jeans instability.

The first magnetic approach came from the hand of Hoyle (1960),[39] who explained that pure viscous effects were not sufficient to prevent a high rotation speed for the star. Instead, magnetic fields coming from the star could transfer sufficient angular momentum to the disk and cause the necessary magnetic braking of the star. Modern theories, like Shu *et al.* (1994),[40] show that the basic angular momentum-loss mechanism for the star is indeed magnetic transfer.

Barge and Sommeria (1995)[41] combined the previous approaches to show that small particles could easily be captured in vortices and lead to the formation of planets. Later, Klahr and Bodenheimer (2003)[42] used hydrostatic simulations to show that, under optimum conditions, disks could create the needed vortices to form planets. Improving understanding of some of these poorly known planet formation processes continues to support many on-going research projects.

Further reading about planet formation history.[43–45]

3.2 | The nebular hypothesis

As mentioned in the previous chapter, stars are born from collapsing clouds through Jeans instability processes. Molecular clouds are not homogeneous structures and therefore they always posses some angular momentum.[36] As compression starts, the conservation of angular momentum forces the surrounding gas to rotate faster. This acceleration pushes the gas away from the collapsing core and facilitates the formation of a gas disk in the equatorial plane.[36,39] The nebular hypothesis states that under certain circumstances, the disk, known as the protoplanetary disk, may give birth to a planetary system. One of the major problems in understanding disk evolution and planet formation is determining how gaseous disks with dust grains evolve into debris disks containing planetary and asteroidal bodies.

Protoplanetary disks are not static arrangements of particles, but rather slowly evolving structures that agglomerate into larger bodies.[46] Although there are sophisticated models to understand this process (*e.g.*[47]), gas and dust in the disk experience drag, settling processes, radial drift, diffusion, Brownian motions and turbulence, which makes detailed study of disks very complicated.

Small solid particles appear to grow by coagulation; collisions cause them to stick together and therefore grow in size.[46] There appears to be no theoretical impediment to the rapid growth of dusty or icy particles up to millimetric dimensions usign this mechanism. The growth of bodies larger than a few millimeters has proved more challenging to model and currently there exists no widely accepted mechanism to explain this process. However, some have speculated about a similar coagulation process working up to planetesimal-size bodies[48] or gravitational instabilities rapidly forming planetesimals from smaller bodies,[49] but none of them provides a complete description of the process.

Once planetesimal-size bodies are formed, the gas disk provides, to a good approximation, only an aerodynamic role.[50] At this stage, further growth is controlled by gravitational interaction between bodies,[50] which can be modeled using Newtonian laws of gravity. Planetesimals colliding and attaching together create larger bodies. This process is well understood and can be reproduced via simulations. The major problem is found when trying to simulate interactions between all the bodies needed to form big systems. For example, $\sim 10^9$ bodies may be needed to recreate the Solar System,[43] a number for which current N-body simulations are infeasible.

Instead, the earliest phases of this stage are simulated using gas-like models that can recreate large amounts of particles. When the number of bodies has dropped, standard simulations can be used to track the evolution of the planets.

Formation of giant planets needs to take into account the gas of the protoplanetary disk once more. Unlike terrestrial planets, most of the giant planets are primarily composed of low-boiling-point materials like gases or ices. Two competing theories purport to explain the formation of those planets. On one hand, a large enough terrestrial planet ($> 10M_{\oplus}$) could acquire a massive gaseous envelop through the accretion of hydrogen from the gas disc.[51] On the other hand, Jeans instability can give rise to fragmentation, allowing smaller overdense regions of the molecular cloud to collapse. If the gas is able to cool in a short time scale it may be possible to directly form giant gaseous planets.[52]

Further reading about the nebular hypothesis.[43–45]

3.3 | Exoplanets detection

The detection of exoplanets is a challenging matter; we know about them because of light perturbations on their host stars or due their thermal radiation emission. Being extremely fainter and only separated by few seconds of arc from their host stars makes direct detection of exoplanets extraordinarily demanding. Most methods rely on the detection of dynamical perturbations that the planet creates on the star.

The first unambiguous exoplanet detection took place in 1992 with the discovery of several terrestrial-mass planets orbiting a highly magnetized, rotating neutron star.[53] In 1995, using radial velocity methods, which are indirect methods of detection that rely on the Doppler effect, Mayor and Queloz (1995)[54] detected a giant planet around a main sequence star. This discovery conceived a new domain of research, and from then, more than 3000 exoplanets have been discovered.

There are five main detection methods for exoplanetary systems. Radial velocity and transit surveys have been the most successful techniques for exoplanetary discovery (in terms of numbers). The radial velocity method was proposed by Struve (1952)[55] when he demonstrated that a very large planet would cause its parent star to exhibit measurable Doppler shifts as the two objects orbit around their center of mass. A detailed study of the Doppler shifts exhibited by the star can also reveal the number of orbiting bodies around the star. Although being an indirect method, 648 exoplanets have been discovered by the radial velocity method according to the open exoplanet catalogue.

Transit detection is by far the most effective discovery method with 2641 exoplanets already identified. To detect a transit it is necessary that the planet is orthogonal to the plane of the sky (*i.e.* the method depends on the planet position with respect to the Earth). If a planet crosses in front of its parent star, the observed light of the star is dropped a small amount (*e.g.* *Figure* 3.1). The amount the star dims depends on the relative sizes of the star and the planet, and if used together with radial velocity methods, they provide an unambiguous determination about the mass and radius of the planet (with respect to the parent star). Density follows from mass and radius, and gives a first estimate of the composition of the planet. Furthermore, during specific times of the transit it is possible to obtain atmospheric photometry and spectroscopy, which provide another insight into the planet's composition.

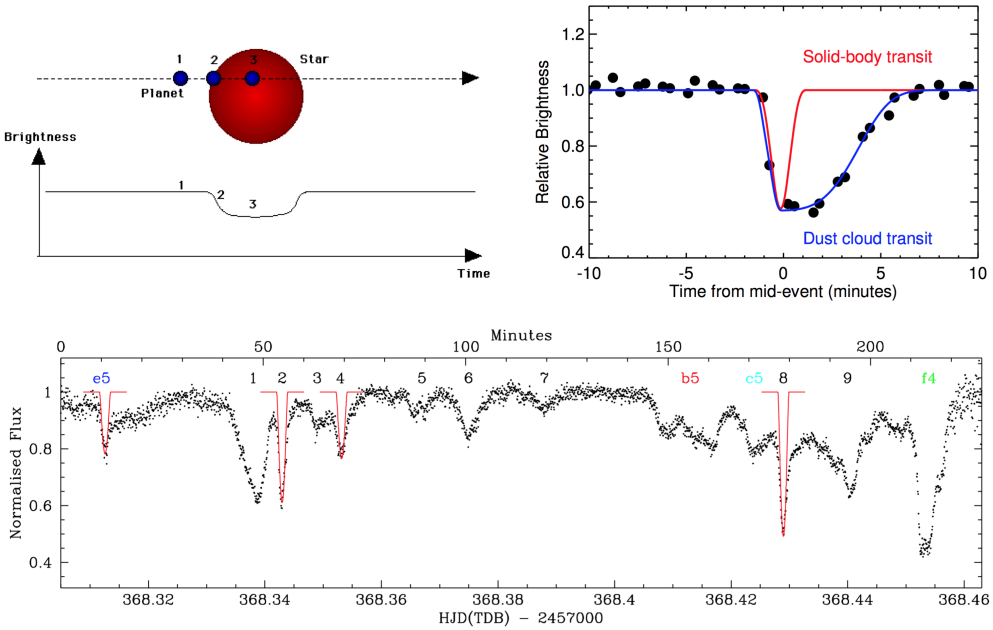

Figure 3.1: The top left panel presents a simplistic representation of a transit event. The top right panel fits one transit event of WD 1145+017 with both a solid-body and a dust-emanating-body. Bottom panel exhibits a normalized flux light curve of WD 1145+017 showing multiple transits. Image credits to Hans Deeg, Vandenburg *et al.* (2015)[56] and Gänsicke *et al.* (2016)[57] respectively.

Direct imaging refers as the detection of light, emitted via infrared thermal emission, of an exoplanet. This technique still faces many challenges, being the most important one blocking the signal coming from the star, which some times can be partially removed or attenuated. This method has managed to detect 48 exoplanets so far.

Among other detection methods, microlensing (40 detected exoplanets) is devoted primarily to very distant systems. The gravitational field of a star can act like a lens and magnify the light of a background star, and planets orbiting the lensing star can enhance or modify the signal. Also, if a system is composed of more than one planet, timing methods (25 detected exoplanets) are very useful. Each planet slightly perturbs the orbits of the others, resulting in measurable time of transit variations.

Further reading about exoplanets detection.[44,58,59]

3.4 | Fate of planets

Despite the uncertainty of how often exoplanetary systems resemble the Solar System, it can provide a starting point for planetary system evolution. As mentioned in the last chapter, the Sun will eventually expand into a giant star and later become a white dwarf. The transformation will force planets to expand their orbits, accrete stellar ejecta and be influenced by solar tidal forces. All these effects, and more not mentioned here, are very difficult to model and therefore they difficult the study of the resulting system.

During the first expansion process of the Sun, Mercury will most likely be engulfed while Venus and the Earth will probably expand their orbits and prevent engulfment.[60] Tidal forces will largely affect and maybe consume Venus[61] while the Earth's fate is a more complex matter. According to Schröder and Smith (2008),[62] the Earth will be engulfed unless all parameters within the evolution model are at the edge of their uncertainty ranges. When the Sun stabilizes into a white dwarf, the remaining Solar System is thought to remain stable and retain more than half of the actual system's mass.[63]

During stellar evolution, the ratio of orbital distance to the star remains constant for all bodies, preventing in this way instabilities. Nevertheless, the change in mass of the star may be enough to make a planetary system become unstable during the post-main sequence evolution of its host star.[64] In this way, the asteroid belt in the Solar System will undergo dynamical instabilities that are likely to force asteroids to orbit eccentrically around the evolved star. In this scenario, highly eccentric bodies can be tidally disrupted if they orbit close enough to the star (*i.e.* inside the Roche radius).

Bonsor *et al.* 2011[65] developed a model for the evolution of planetesimal structures like the Neptune-Kuiper belt. They showed that an important fraction of the mass remains orbiting the the evolved star and that enough mass is engulfed by the star to pollute its atmosphere. The atmospheres of white dwarfs are easier to study than exoplanets or belts of asteroids, thus, a proper atmospheric study can give information about the actual orbiting system as well as the one that used to orbit the main sequence star.

Further reading about planetary fate.[66,67]

4

Circumstellar disks

4.1 | Circumstellar disks

Circumstellar disks are flattened, ring-shaped structures of matter, usually gas and dust, in orbit around a star. The fact that they are almost confined to the plane of stellar rotation distinguishes them from spherical clouds or envelopes. Disks orbit stars at various stages of their evolution life cycles. As seen in Chapter 2 stars are formed from a collapsing cloud of matter. When the pre-main sequence star is composed, the cloud is already flattened creating a disk that is thought to be related to the creation and existence of planets (see Chapter 3). As the star evolves so does its disk. Mature, main-sequence stars exhibit dusty disks created by collisions of smaller bodies such as asteroids or planetesimals. After stars have evolved beyond the main sequence, the nature of their orbiting disks is more complicated to understand and often still an unexplained phenomena.

Circumstellar, dusty disks around main-sequence stars were first discovered by the infrared satellite (IRAS) in 1983. Some bright stars emitted much more radiation at the infrared range than the stellar photosphere can produce. This infrared excess is usually associated with the presence of dust particles. Absorbing optical and ultraviolet light from the star, dust particles are able to re-radiate light back in the infrared range.[46,68] Although most of the detected material consists of small dust particles, a few stars also show evidence of gas in their circumstellar disks (*e.g.*[69,70]). While dust particles are thought to be linked with the formation of rocky bodies, gas might be related to giant gassy planets.[69]

The Sun itself has a circumstellar disk that can be thought of as the whole Solar System without the planets, formed in this way mainly by the Asteroid and Kupier belts. The Sun's circumstellar disk is used as a model for most of the observed disks in other stars. While circumstellar disks around main-sequence stars, like our Sun, can provide insight on planet formation, when orbiting more evolved stars like white dwarfs they might open a new door to the understanding of their previous planetary systems.[71]

The Universe is highly bright in the infrared, which makes disk detections very difficult. Circumstellar dust orbiting white dwarfs has been historically hard to distinguish, and even today, disks around these stars are extremely challenging to study. The complexity arises mainly for two reasons: (i) the radiation of the disk is proportional to the luminosity of the star, and white dwarfs are around 10^{-4} less luminous than their main-sequence counterparts, and (ii) the observed excess might not come from the white dwarf disk but from companion stars that can easily outshine the white dwarf in the infrared.[72]

Over the last two decades, hundreds of white dwarfs have been surveyed for infrared excess due to circumstellar disks.[73] The first white dwarf with an infrared excess was identified by Zuckerman and Becklin (1987)[74] and was later confirmed to posses a dusty circumstellar debris disk by Graham *et al.* (1990).[75] The discovery of the second dusty white dwarf came a decade later[76,77] and to date, debris disks have been detected orbiting nearly 40 white dwarfs (*e.g. Figure* 4.1).

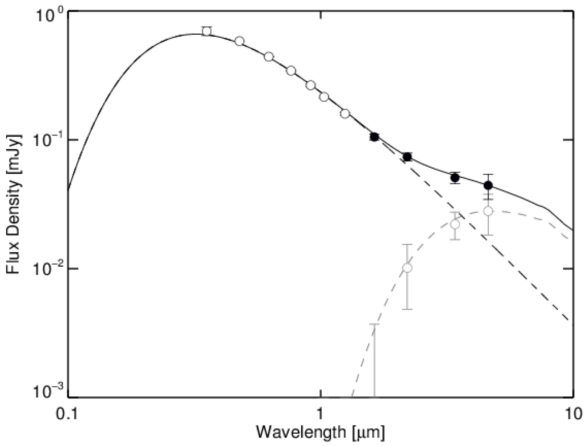

Figure 4.1: WD 1145+017 photometric excess evidencing the presence of a circumstellar debris disk. White data points show non- excess measurements, whilst black data points denote wavebands with excess emission. From Zhou *et al.* (2016).[78]

Further reading about circumstellar disks.[67,79]

4.2 | Disks and metal pollution

To provide a complete review of the relevance of circumstellar disks orbiting white dwarfs, it is necessary to introduce the concept of atmospheric metal contamination. Because of their nature, white dwarfs are $\sim 10^5$ times as dense as the Sun. Consequently, due their strong gravitational field, the atmospheres of white dwarfs quickly separate light elements from heavy ones.[80] Lighter elements (*i.e.* hydrogen and helium) can be found in the top layers, which yields the main classification groups DA and DB (see Chapter 2). Metals (elements more massive than H or He other than C) sink really quickly ($\sim< 10^6$ years) in these environments and it is impossible to detect them in the interiors of white dwarfs via spectroscopy. Therefore, white dwarfs that are older than a few tens of mega-years should have atmospheres which are composed of a combination of hydrogen, helium and carbon only (this last one coming from the carbon-rich nucleus). Nevertheless, some old white dwarfs exhibit strong traces of metals in their atmospheres.

There are two possible origins for the atmospheric metal traces observed in white dwarfs: accretion from the interstellar medium or accretion from a remnant planetary system. In both cases the most probable scenario is that the accretion is facilitated by a circumstellar disk from which the white dwarf continuously renews its metal supply. No confidently reported debris disk around a single unpolluted white dwarf exists, suggesting a link between pollution and disks. At least a few percent, and up to all white dwarfs, host circumstellar disks.[81,82]

Accretion from the interstellar medium was the most widely accepted theory to explain metals in white dwarfs. The model predicts that white dwarfs can accrete enough material to pollute their atmospheres when going through dense regions of the interstellar medium. Nevertheless, this approach faces two major obstacles. The first one is that, using proper motion studies, it is possible to know the past trajectory of the star, and in many cases, white dwarfs showing the presence of metals did not go though any reasonably dense cloud of interstellar medium. The second problem comes when trying to explain DBZ white dwarfs, which show metals traces but no sign of hydrogen in their atmospheres. Because the interstellar medium is composed mainly of hydrogen, metal polluted white dwarfs should also be accreting hydrogen and therefore present a hydrogen-rich atmosphere.

Nowadays, a planetary origin for the metal pollution is the accepted theory. This model states that the metals are accreted from a remnant planetary system that survived the evolution of the star. In this way, asteroids, planetesimals or planets are engulfed by the white dwarf providing a reservoir of metals. There is plenty of evidence supporting this suggestion. Debris disks, which are likely formed through orbiting disrupted bodies, are always found around metal polluted white dwarfs. Also, the chemical abundances of white dwarf's atmospheres are very similar to the bulk composition of planetesimals orbiting our solar system (*e.g.*[83]). Finally, there have been recent observations of rocky bodies disintegrating around a metal polluted white dwarf.[56]

The existence of a remnant planetary system also aids with the explanation of detected debris disks. The observed compact debris disks around white dwarfs cannot have formed during the pre-white dwarf stage of the star because they would have been engulfed during the red-giant phase. Also, because of their age and composition disks cannot have formed due to interstellar fallback as metals would have been already accreted. This yielded the currently accepted prediction to be that those disks are formed from the disruption of bodies around the star.[71,84] These bodies, expected to orbit eccentrically, can be disrupted by tidal forces and create a dusty debris disk around a white dwarf from which to accrete enough metals to explain its metal pollution.[85]

Further reading about disks and metal pollution.[67,86]

5

WD 1145+017

5.1 | Relevance

Previous chapters 2, 3 and 4 provide necessary background to understand a basic description of the white dwarf WD 1145+017 and its system. The aim of this chapter is to present the importance of this white dwarf and provide a review of the research performed on the system.

Chapter 2 illustrates that white dwarfs are extremely dense objects usually classified by abundances in their atmospheres. Between 25 and 50% of all white dwarfs cooler than 20,000 K exhibit the presence of elements heavier than hydrogen or helium in their atmospheres.[87–89] Due to the density of the star, these elements quickly (compared to their cooling times) sink beneath the outer layers of hydrogen and/or helium. The detection of metals in white dwarfs atmospheres implies that heavy materials were recently deposited onto the surfaces of these stars (*e.g.*[88,89]).

Although it was suggested that this material originated from the interstellar medium and was acreted to the star (*e.g.*[90]), there were many problems with this theory. High-resolution observations of these polluted white dwarfs display metal abundances similar to the ones of solar system objects,[91] which helped with a new approach. The currently accepted origin for these elements is that they come from massive rocky bodies that have been orbitally perturbed and tidally disrupted by the star.[64] Then, material from these bodies accretes onto the white dwarf.[71,88]

Chapter 3 explains that planets around main-sequence stars are rather common[92,93] and that some of them are thought to keep orbiting the star during its white dwarf transformation.[94,95] It also reviews the current detection mechanisms for exoplanets and how difficult it is to detect them.

Chapter 4 describes how rocky bodies can be responsible for the creation of dusty circumstellar debris disks around post main-sequence stars. These debris disks are thought to be an accretion mechanism for white dwarfs, linking the presence of metals in their

atmospheres to circumstellar material near the star's tidal disruption radius for rocky material.[73,81,96,97] Dusty debris disks have been found around many of these polluted white dwarfs by detecting an infrared excesses.[74,96]

The current accepted explanation for these observations is that the mass loss associated with the white dwarf transformation destabilizes the original planetary system to the point that rocky bodies get close enough to the white dwarf for tidal disruption. Hence, those fragmented bodies create a debris disk capable of polluting the white dwarf's atmosphere.[64,85,98,99]

Many white dwarfs have been found to exhibit metals in their atmospheres and dusty or gaseous disks, but despite the efforts of many research groups, it was not until recently that a white dwarf with transiting bodies was observed. The *K*2 (second generation Kepler) mission light curve of WD 1145+017 showed transits of variable depth with several distinct periods around 4.5 h.[56] WD 1145+017 also has a significantly polluted spectrum and displays an infrared excess, for this reason, WD 1145+017 might be a perfect example of a white dwarf accreting material from planetesimals.

The fact that the disruption is currently happening gives us an unique opportunity to study the planetesimal properties before they are totally accreted onto the star.[85] Although the excitement of finding an scenario like this for the first time, this appears to still be an incomplete picture of the system which demands further research.

5.2 | History

WD 1145+017 (also designated EPIC 201563164) was first identified by Berg *et al.* (1992).[100] The observations from the Large, Bright QSO Survey (LBQS) revealed the helium-rich atmosphere (DB) of the white dwarf. Together with WD 1145+017, Berg *et al.* classified 20 more white dwarfs, 9 of them also DB. Later on, with the findings of Hamburg/ESO survey, Friedrich *et al.* (2000)[29] studied 40 cool ($T_{\rm eff}$ < 20.000 K) helium-rich white dwarfs. As WD 1145+017 is among them, Friedrich *et al.* used a helium-atmosphere model to provide a first estimate for its effective temperature of $T_{\rm eff}$ ~ 17.000 K. At that epoch the star was only known to be an ordinary helium envelope white dwarf.

Vanderburg *et al.* (2015)[56] were the first to observe the transits that would make WD 1145+017 the first of its kind. The 17 *Kepler*-band magnitude star showed at least one, and provably several, deep transits in its *K*2 (second-generation Kepler) light curve. Vanderburg *et al.* (2015)[56] performed a periodogram analysis to search for periodic signals equivalent to orbiting bodies. One strong peak was found at a period of 4.499 h together with five other weaker, but statistically significant, signals at periods between 4.5 and 5 h. In order to confirm the transits, Vanderburg *et al.* (2015)[56] also performed ground observations of WD 1145+017's transits.

WD 1145+017 has a dusty debris disk, and the star's spectrum showed prominent lines from heavy elements. Using photometry from the Sloan Digital Sky Survey (SDSS) and a metal-polluted atmosphere model, Vanderburg *et al.* (2015)[56] obtained a refined measurement for WD 1145+017's effective temperature of $T_{\rm eff} = 15.900 \pm 500$ K. Vanderburg *et al.* (2015)[56] also estimated the mass ($0.6 M_\odot$), radius ($1.4 R_\oplus$) and cooling age (175 ± 75 Myr) of the white dwarf.

A detailed analysis of the transits revealed that their shapes were not consistent with completely solid objects. Vanderburg *et al.* (2015)[56] interpreted the transits' elongated form as the evidence of dusty tails emanating from rocky objects. By assuming a stellar mass of $0.6 M_{\odot}$, Vanderburg *et al.* (2015)[56] calculated the disintegration (or Roche) radius for a common rocky asteroid. Since the observed transits felt inside this radius, Vanderburg *et al.* (2015)[56] interpreted the events as disintegrating planetesimals orbiting the white dwarf. Vanderburg *et al.* (2015)[56] also estimated the mass-loss rate from the planetesimals necessary to explain the transits of WD 1145+017 with dusty tails ($\sim 8 \times 10^9\,\mathrm{g\,s^{-1}}$). Furthermore, because of the circumstellar debris disk and the metal pollution, Vanderburg *et al.* (2015)[56] proposed that the system was the first detection of planetesimals acting as the main pollution mechanism for a white dwarf.

Soon after, Croll *et al.* (2015)[101] provided multi-wavelength, multi-telescope, ground-based follow-up photometry of the white dwarf. Croll *et al.* (2015)[101] confirmed the existence of orbiting bodies around WD 1145+017 and reported 9 different significant dips in photometric flux. The transit egress timescale being usually longer than the ingress timescale added further corroboration to the hypothesis of cometary tails streaming behind the orbiting objects. Croll *et al.* (2015)[101] also constrained the size of the emanating particles to be $\sim 0.15\,\mu$m or larger, because no difference in the transits was observed between the V- and R-bands.

Xu *et al.* (2015)[83] observed WD 1145+017 with the High Resolution Echelle Spectrometer (HIRES) and discovered numerous circumstellar absorption lines that were also present in the atmosphere of the star. With this discovery, Xu *et al.* (2015)[83] stated that we were witnessing the active disintegration and subsequent accretion of an extrasolar asteroid. Xu *et al.* (2015)[83] also calculated a minimum of already accreted mass (6×10^{23}g) to the star which lead them to suggest that WD1145+017 was in a very early stage of tidal disruption and it was experiencing a high-accretion burst, translating into mass loss rates up to $10^{13}\,\mathrm{g\,s^{-1}}$.

Using high-speed photometry, Gänsicke *et al.* (2016)[57] revealed the system's evolution since Vanderburg's *et al.* (2015)[56] findings. New observations presented dynamic transits changing size and shape in a matter of days. Some transit signals were dissipated, while others appeared suddenly, some exhibited sharp ingresses and broad egresses, and vice versa. Gänsicke *et al.* (2016)[57] found the strongest periodic signal at 4.498 h which was in agreement with Vanderburg's *et al.* (2015)[56] analysis. Nevertheless, the weaker signals appeared in slightly shorter orbital periods. Gänsicke *et al.* (2016)[57] provided detailed orbital period measurements for 6 almost co-orbital objects (with a mean period of 4.4930 h) that lead to the hypothesis of a parent body orbiting at 4.498 h and several tidally disrupted fragments orbiting at shorter orbits. Also, due the rapid variability of the observed transits, Gänsicke *et al.* (2016)[57] estimated a $10^{13}\,\mathrm{g\,s^{-1}}$ mass loss rate for the planetesimals, which lay between the values reported by Vanderburg *et al.* (2015)[56] and Xu *et al.* (2015).[83]

Taking a similar approach, Rappaport *et al.* (2016)[102] analyzed WD 1145+017's transits to track up to 15 different fragment transits. Some of these bodies vanished in a matter of days while others appeared all of a sudden. Rappaport *et al.* (2016)[102] found the strongest signal at a slightly longer period of 4.5004 h (compared to the 4.498 h previously found). Rappaport *et al.* (2016)[102] plotted the transits folded in a 4.5004 h period to exhibit how almost all objects drift systematically in phase with respect to the parent body. By performing a theoretical study of planet disruption, Rappaport *et al.* (2016)[102] demonstrated how lower-orbit bodies could be fragments coming from the body orbiting at 4.5004 h. Furthermore, Rappaport *et al.* (2016)[102] predicted, with a theoretical approach, the mass for the parent body to be near 10% the mass of Ceres.

Alonso *et al.* (2016)[103] observed several relatively deep transits with the Gran Telescopio Canarias (GTC). In order to place stronger constraints on the sizes and compositions of the occulting material, Alonso *et al.* (2016)[103] dispersed the observation spectrum into 4 bands centered at 0.53, 0.62, 0.71, and 0.84 μm. After normalization, Alonso *et al.* (2016)[103] compared the flux light curves of all the bands to find no notable difference between them. The remarkable non-chromaticity lead to the conclusion that dust grains should be bigger than 0.5 μm for most common minerals.

In a similar vein, Zhou *et al.* (2016)[78] performed near-infrared and visible observations of WD 1145+017. By increasing the wavelength range compared with previous studies, Zhou *et al.* (2016)[78] revealed that both light curves were consistently the same, allowing a stronger constraint in the size of the particles, which should be bigger than 0.8 μm. This particle size is consistent with the infrared excess of the white dwarf and suggests a debris disc created mostly due to collisions.

Until now, despite the mentioned investigations, it has not been possible to robustly constraint parameters like the mass or eccentricities of the lower-orbit bodies. The fact that those magnitudes are unconstrained to within many orders of magnitude impedes us from obtaining information about processes like disruption and subsequent accretion onto the star, which are happening in the WD 1145+017 system.

6

Simulation set up

6.1 | Motivation

With its unique nature, WD 1145+017 can help us shed some light on planetesimals processes which are still poorly understood. Observations of this star have revealed the presence of one parent body orbiting at a period of $\sim 4.5\,\mathrm{h}$ and at least six fragments orbiting at shorter ($\sim 4.49\,\mathrm{h}$) and constant periods (over $\sim 550\,\mathrm{days}$). However, to accurately describe the behaviour of the planetesimals around this white dwarf it is necessary to improve the current constraints on their masses and eccentricities. This work approaches the system from a computational point of view. In contrast to what observed, N-body simulations of the system show that, under specific configurations, planetary fragments abandon their observational orbital periods. A computational approach can therefore provide new insights into the stability and evolution of planetesimals around white dwarfs.

6.2 | Mercury Code

This work uses John E. Chambers' (1999)[104] Mercury as a numerical integrator to simulate the dynamics of the system orbiting WD 1145+017. Mercury code is a Fortran package which specializes in modelling planetary dynamical evolution. The code was created with the aim to offer a versatile way of studying the long-term stability of planetary systems and modelling the orbital evolution of different celestial bodies. Mercury is designed to understand both Cartesian and Keplerian elements and offers the possibility to use different numerical integrators to monitor the trajectories of the bodies. Mercury also records details about close encounters, ejections and collisions between objects.

MERCURY uses a set of "in" files which define the integration behaviour and produces a corresponding set of "out" files containing the trajectories and the results of the integration:

In files are text documents that determine the initial conditions of all bodies and the way the code should perform the numerical integration. Usual configuration of MERCURY includes "Big.in", "Small.in", "Param.in" and "Element.in" files.

- **Big.in:** The Big.in file contains the initial conditions of all bodies which are considered massive. These bodies are the ones which would have a gravitational impact on other objects. Initial conditions are the position and velocities of the bodies (if using Cartesian coordinates) or the asteroidal components (if using Keplarian coordinates) at the beginning of the integration. This work considers all bodies as massive bodies.

- **Small.in:** The Small.in file contains the initial conditions of all bodies considered not massive. Not massive bodies are the ones that despite being affected by gravity do not have an effect on other bodies. Initial conditions are specified in the same way as in Big.in.

- **Param.in:** The Param.in file regulates the way the integration is going to be performed. The file sets which integrator will be used (Bulirsh-Stoer (BS) , mixed-variable symplectic or a hybrid integrator), the time-step for the integrator (BS uses an automatic time-step), the length of the simulation (in days), the accuracy parameter and the variables that describe the central body (mass and radius of the central star).

- **Element.in:** The Element.in file determines the format of the output files. This file defines whether the output trajectories of the bodies will be given with respect to a fixed central body in the origin (no orbital motion of the central star) or with respect to the barycentric point fixed in the origin (accounting for orbital motion of the central star). Element.in also establishes the interval between outputs (how often a point is added to a trajectory) and all the trajectory parameters to be printed out at each output time-step.

Out files are text documents produced after the numerical integration. These files contain information about the trajectories and interactions between the bodies. Usual configuration of MERCURY includes "Body.aei" and "Info.out" files.

- **Body.aei:** Body.aei files are a set of documents containing the details of each body's trajectory. For each output time-step the file shows the values for all the trajectory parameters defined in the "Element.in" file . There is one ".aei" file for each body.

- **Info.out:** The Info.out file contains a summary of the simulation. It shows the error introduced by the integrator in terms of fractional energy change [AU^2 $days^{-2}$] and angular momentum change [AU^2 $days^{-1}$] of the system. It also shows the interactions between bodies, which include close encounters (one body orbits close to another), collisions (one body hits another one or the star) and ejections (one body goes out of the simulation spacial domain).

The code used in this work is an slightly modified version of MERCURY which includes some adjustments to better implement the effects of general relativity and to improve the collision detection mechanism (for details see Veras *et al.* (2013)[95]).

6.3 | Automatizing

The aim of this work is to simulate many different possible scenarios for the system WD 1145+017 and compare their evolution with observations. For our initial conditions we assume 6 co-orbital lighter bodies and a larger one orbiting a white dwarf with a mass of $0.6M_{\odot}$ and a radius of $1.4R_{\oplus}$.

In order to accurately model interactions between planetesimals (a necessity for this study) we use the Bulirsch-Stoer (BS) integrator which yields the best precision. This integrator features an adaptive time-step, which is determined by a tolerance parameter given at the start of the simulation. A tolerance of 10^{-12} is considered to be highly accurate[105] and, therefore, we adopt it for these simulations. As a safety check, some of the simulations are also run again with an accuracy parameter of 10^{-13}.

In this work we aim to constrain the mass and the eccentricity of all the orbiting bodies. Under the assumption that the lighter bodies are are tidally disrupted fragments of the same parent body, we constraint the mass of the fragments to be between 0.01% and 20% of the parent body mass. For each simulation, every fragment is assigned a different and random value of mass within the specified range. Also, because no spatial configuration can be resolved by observations, our simulations include initial mean anomalies drawn from a uniform random distribution.

The fact that fragments have been in the same orbits for at least $\sim$ 550 days suggests that they have low eccentricities because tidal disruption is a strong function of orbital pericentre and almost independent of semimajor axis.[85]

Assuming no eccentricity for the fragments, the only parameters left to define are the mass of the parent body and its eccentricity, henceforth (M,e) pair. In this work we sample permutations of (M,e) pairs and compute the evolution of the fragments over a time-span of 2 or 5 years. Because of the big number of (M,e) pairs and the fact that more than 50 simulations are performed per each (M,e) pair, an automatizing method was essential.

Because of the author's experience in Matlab, the automatizing method is coded using this language. The code creates a copy of the MERCURY package in a new folder with a specific name highlighting the special features it will contain ((M,e) pair and number of simulation). All the In Files in the folder are then automatically modified just before running the Fortran MERCURY code. After the integration is completed, the code analyses the results and either performs changes in the current simulation or proceeds with the next one. The automatized algorithm has to handle 3 different coding languages (Matlab, Fortrant and Bash), deal with large amounts of data and distribute tasks to different computers in order to decrease computation time.

7

Results

7.1 | Mass and eccentricity constraints

All the results obtained are presented in the following paper, which has already been submitted to MNRAS (Monthly Notices of the Royal Astronomical Society). The paper includes sections such as “Introduction”, “WD 1145+017 system” and “Simulation setup” that are also included and covered more detailedly in this work.

MNRAS **000**, 1–7 (2016) Preprint June 2016 Compiled using MNRAS LATEX style file v3.0

Mass and eccentricity constraints on the planetary debris orbiting the white dwarf WD 1145+017

Pol Gurri,[1,2]⋆ Dimitri Veras,[2] and Boris T. Gänsicke[2]
[1] *Departament de Física, Universitat Politècnica de Catalunya, c/Esteve Terrades 5, 08860 Castelldefels, Spain*
[2] *Department of Physics, University of Warwick, Coventry CV4 7AL, UK*

June 2016

ABSTRACT
Being the first of its kind, the white dwarf WD 1145+017 exhibits a complex system of disintegrating debris which offers a unique opportunity to study its disruption process in real time. Even with plenty of transit observations there are no clear constraints on the masses or eccentricities of such debris. Using N-body simulations we show that masses greater than $\simeq 10^{20}$ kg (a tenth of the mass of Ceres) or orbits that are not nearly circular (eccentricity $> 10^{-3}$) dramatically increase the chances of the system becoming unstable within two years, which would contrast with the observational data over this timespan. We also provide a direct comparison between transit phase shifts detected in the observations and by our numerical simulations.

Key words: minor planets, asteroids: general – stars: white dwarfs – methods:numerical – celestial mechanics – planet and satellites: dynamical evolution and stability – protoplanetary discs

1 INTRODUCTION

Planets which survive the giant branch evolution of their hosts stars are expected to be rather common (Burleigh et al. 2002; Villaver & Livio 2007; Mustill & Villaver 2012; Veras et al. 2013). This prediction is corroborated by the detection of photospheric metal pollution in a large fraction of all white dwarfs (Zuckerman et al. 2003, 2010; Koester et al. 2014). Dynamical interactions in evolved planetary systems can scatter planetary bodies near the Roche radii of the white dwarfs (Debes & Sigurdsson 2002; Frewen & Hansen 2014a; Payne et al. 2016) where they are tidally disrupted (Jura 2003; Debes et al. 2012c; Veras et al. 2014a, 2015b), forming detectable accretion discs (Zuckerman & Becklin 1987; Gänsicke et al. 2006; Kilic et al. 2006; Farihi et al. 2009; Bergfors et al. 2014), and ultimately accreting onto the white dwarf. Analysis of the photospheric trace metals provides detailed insight into the bulk chemical compositions of planetary systems (Zuckerman et al. 2007; Gänsicke et al. 2012; Xu et al. 2014), which in turn guides planet formation models (e.g. Carter-Bond et al. (2012)). The current observational and theoretical progress on evolved planetary systems is summarised by Farihi (2016) and Veras (2016).

Vanderburg et al. (2015) announced transits recurring on a period of $\simeq$ 4.5 h in the $K2$ light curve of the white dwarf WD 1145+017, which also exhibits infrared excess from a circumstellar disk and photospheric metal pollution. The orbit of the transiting objects lies close to the disruption, or Roche, limit for rocky objects. Thus, WD 1145+017 represents the first observational detection of planetesimals orbiting a white dwarf, opening a new window into the understanding of poorly-known processes such as disintegration, orbital circularisation, or the actual nature of those orbiting bodies (Veras et al. 2015c,d; Veras 2016).

In this work we derive constraints for the masses and eccentricities of the bodies orbiting the star from N-body simulations of the system. Section 2, provides an overview of the WD 1145+017 system and Sect. 3 outlines the setup of our simulations. In Sect. 4 and 5 we present the results that set constraints on the mass and eccentricity of the orbiting debris. Section 6 is devoted to phase shifts, proving also a direct comparison between observational data and our simulations.

2 WD 1145+017 SYSTEM

The 17th magnitude white dwarf WD 1145+017, first identified by Berg et al. (1992) and rediscovered by Friedrich et al. (2000), was observed during Campaign 1 of the extended *Kepler* mission, and Vanderburg et al. (2015) discovered transits of at least one, and probably several, bodies with periods ranging from 4.5 h to 4.9 h in the *K2* light curve. Deep ($\simeq$ 40%) transits lasting $\sim$ 10 min recurring every 4.5 h (near the Roche-limit for a rocky body) were confirmed in ground-based follow-up photometry, which Vanderburg et al. (2015) interpreted as dust and gas emanating from a smaller, undetected object, analogous to a cometary tail (Vanderburg et al. 2015). Optical spectroscopy revealed both photospheric metal pollution (Vanderburg et al. 2015) and absorption from cir-

⋆ E-mail: polgurri@gmail.com

cumstellar gas (Xu et al. 2016), and an infrared excess detected in the UKIDSS and *WISE* photometry confirmed the presence of circumstellar dust (Vanderburg et al. 2015).

High-speed photometry obtained by Gänsicke et al. (2016) over the course of 15 nights in November and December 2016 revealed the rapid evolution of the system since the discovery by Vanderburg et al. (2015). Multiple transits typically lasting 3 – 12 min and with depths of 10 – 60% were observed on every occasion. While these transit events changed depth and shape on time scales of days, Gänsicke et al. (2016) could track six individual features over at least three individual observing nights, and concluded that at least six objects were orbiting WD 1145+017 on nearly identical orbits, with a mean period of 4.4930 ± 0.0013 h. This period is significantly distinct, and shorter, compared to the dominant 4.5 h period measured by Vanderburg et al. (2015) from the *K2* data. A few transits with similarly short periods were also detected by Croll et al. (2015).

Additional extensive photometry obtained with small-aperture telescopes confirmed the presence of multiple objects with periods of $\simeq 4.493$ h, as well as the 4.5 h period detected in the *K2* data (Rappaport et al. 2016). Comparing these two distinct periods, Rappaport et al. (2016) used an analytical model in which fragments drift off a Roche-lobe filling asteroid to estimate the mass of the asteroid to be $\simeq 10^{20}$ kg, about one tenth of the mass of Ceres. In the context of this paper, we will refer to the object at $\simeq 4.5$ h as the *parent body*, and to the multiple objects with periods of $\simeq 4.493$ h as *fragments*.

The physical nature of the obscuring material has been investigated by Alonso et al. (2016) who obtained spectroscopic transit observations through a wide slit. Binning their data into four bands centred at 0.53, 0.62, 0.71, and 0.84 μm, Alonso et al. (2016) found practically no colour-dependence of the transit shapes and depths, and concluded that the particle size of the debris must be $\gtrsim 0.5\mu$m. More recently, Zhou et al. (2016) obtained multi-band photometry spanning $0.5 - 1.2\mu$m using several telescopes, and derived a 2σ lower limit on the particle size of 0.8μm.

Several estimates of the current accretion rates were derived from the dust extinction ($\simeq 8 \times 10^6$ kg s^{-1}, Vanderburg et al. 2015; $\simeq 10^8$ kg s^{-1}, Gänsicke et al. 2016) and the gas absorption lines ($\simeq 10^9$ kg s^{-1}, Xu et al. 2016). The metal content of the white dwarf envelope is $\simeq 6.6 \times 10^{20}$ kg (Xu et al. 2016), however, given that the time scales on which the metals diffuse out of the envelope are a few 10^5 yr, it is not possible to unambiguously associate that metal content with the ongoing disruption event.

3 SIMULATION SETUP

Our N-body numerical simulations are based on a model of WD 1145+017 that, while taking into account the results from the recent follow-up observations, ignores the detailed process of the tidal disruption of the bodies orbiting the white dwarf (Debes et al. 2012a; Veras et al. 2014a), as well as effects such as collisions and interactions with the debris disk, white dwarf radiation (Veras et al. 2015c,a,d) or gas drag (Veras et al. 2015a,b) which may play an important role in the evolution of the system. The study of Veras et al. (2016a) considered only equal-mass bodies in initially strictly co-orbital configurations, an approach which is unsuitable for WD 1145+017. We rather intend to provide understanding of many-body interactions specifically for the system harbouring WD 1145+017.

All simulations are performed using the N-Body code Mercury (Chambers 1999) with some extra modifications which include the effects of general relativity and improve the collision detection mechanism in the same way as used by Veras et al. (2013). Our simulations record the interactions between bodies for a duration of at least two years, spanning approximately the observational baseline. We use a BS (Bulirsch-Stoer) integrator with an accuracy parameter of 10^{-12}. For every set of simulations, a subset of them are re-run with a smaller accuracy parameter of 10^{-13} and results are double-checked using both Cartesian and Keplerian coordinates.

Each simulation recorded the interactions between a parent body at an orbital period of 4.498h and six fragments at 4.493 h orbiting a $0.6M_\odot$ and $1.4R_\oplus$ white dwarf like WD 1145+017 (Vanderburg et al. 2015). The lack of strong observational evidence supporting any specific orbital configuration for the bodies motivated us to randomly sample from a uniform distribution the initial mean anomalies for all bodies and simulations. Also, under the hypothesis of the fragments being tidally-disrupted parts of the parent body, we assumed their masses to range from 0.01% to 20% of the parent body's mass, and we lineally randomised the masses of all fragments for every simulation between those values. Therefore, the only free, non-random parameter in our simulations was the mass of the parent body.

4 MASS CONSTRAINTS

Being able to obtain an order-of-magnitude constraint on the mass of the bodies was the first motivation of the simulations. Observations suggest that the planetesimal(s) at WD 1145+017 have been in the same, or very similar, orbits for at least ~ 500 days (Gänsicke et al. 2016) and therefore should have low eccentricities (tidal disruption strongly correlates with orbital pericentre instead of semi-major axis (Veras et al. 2015c), meaning that highly eccentric orbits would cause a rapid disruption of planetesimals). Thus, we imposed completely circular orbits for all bodies and ran simulations for an extended time of five years to gain insight into the time scale on which the system evolves. We gradually increased the parent body's mass, using 10 linearly-distributed values per decade in mass, from $\sim 10^{18}$ kg to $\sim 10^{21}$ kg and performed 100 simulations for each mass value. As a result, we obtained detailed trajectories for all bodies over time, allowing us to track changes in their orbital periods.

Interactions between bodies can cause observationally measurable deviations in the orbital periods (Veras et al. 2016a). Therefore, we monitored the difference that each body experienced between its orbital period during the simulation, $T(t)$, and its initial orbital period, $T(0) = 4.493$ h, which we will refer as $\Delta T(t) = T(t) - T(0)$. For each simulation, we only kept the maximum value of $\Delta T(t)$ among six fragments, $\Delta T_{\rm max}$ (see Figure 1). Performing 100 simulations for each value of parent body's mass yielded an average maximum period deviation $\langle \Delta T_{\rm max} \rangle$ which depended only on the mass of the parent body.

$\Delta T_{\rm max}$ provides insight into the stability of the system. Large values of $\Delta T_{\rm max} \gtrsim 20$ s translates into fragments being greatly affected by the parent body and experiencing potentially detectable changes in their orbital periods. With the periods of the fragments and the parent body being initially separated by $\simeq 30$ s, period deviations up to 60 s resulted in some simulations where fragments entered new orbits around the parent body! In contrast, small period deviations imply a low level of interaction between bodies and a greater chance of long-term dynamical stability.

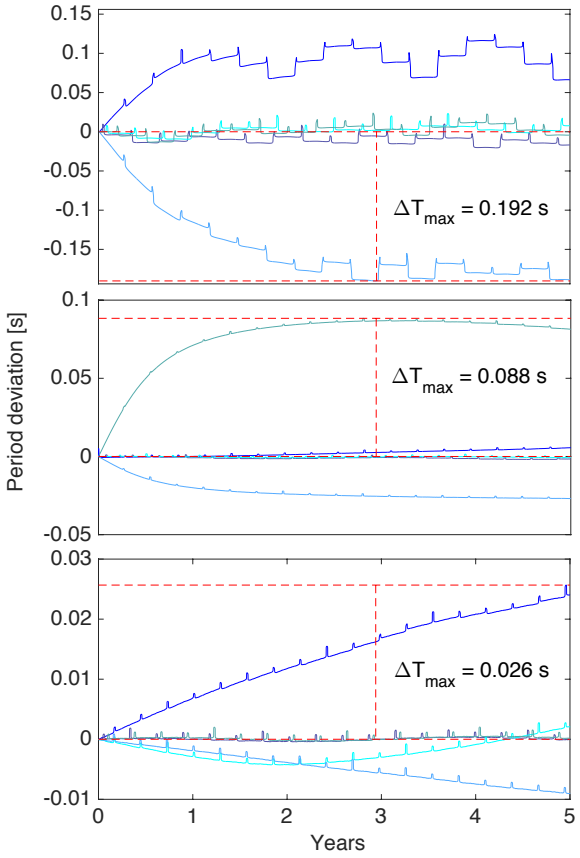

Figure 1. Each line represents the period deviation $\Delta T(t) = T(t) - T(0)$ of a fragment as a function of time. Three different simulations are shown to help visualize the complex behaviour of fragments' trajectories and to illustrate our definition of the period deviation $\Delta T_{\max}$. The mean $\langle \Delta T_{\max} \rangle$ is computed as the average of all values of $\Delta T_{\max}$, while $\mathrm{Max}(\Delta T_{\max})$ and $\mathrm{Min}(\Delta T_{\max})$ are the highest and lowest values among all $\Delta T_{\max}$.

Figure 2 plots $\langle \Delta T_{\max} \rangle$ with respect to the mass of the parent body. Grey lines give the dispersion of the obtained $\Delta T_{\max}$ measures. The vertical blue dashed line is the Rappaport et al. (2016) theoretical prediction for the mass of the parent body and the horizontal blue dashed line is representing the maximum difference between the observed orbital periods and their mean (Gänsicke et al. 2016).

Although the maximum difference between the observed orbital periods and their observational mean (horizontal blue dashed line in Figure 2) does not directly relate with period deviation, it provides a sense of how radially distant are fragment's orbits in stable configurations. Because no fragment has been observed further than $\simeq$ 8 s away from the mean orbital period, it can set an order-of-magnitude upper limit for $\langle \Delta T_{\max} \rangle$. One caveat is that a large $\Delta T_{\max}$ can be generated by one fragment alone, which might be undetectable observationally. We should also note that although observations suggest a nearly constant orbital period of the fragments over $\simeq$ 500 days, $\Delta T_{\max}$ in our simulations is computed over five years. We aimed to reduce these uncertainties by averaging over 100 simulations.

Figure 2 shows a clear positive correlation between $\langle \Delta T_{\max} \rangle$ and the parent body's mass, with the strongest dependence occurring between 5×10^{19} kg and 2×10^{20} kg and then levelling off at about 5×10^{20} kg. Assuming that $\langle \Delta T_{\max} \rangle$ has to be less than the difference between the observed orbital periods and their mean, this sharp

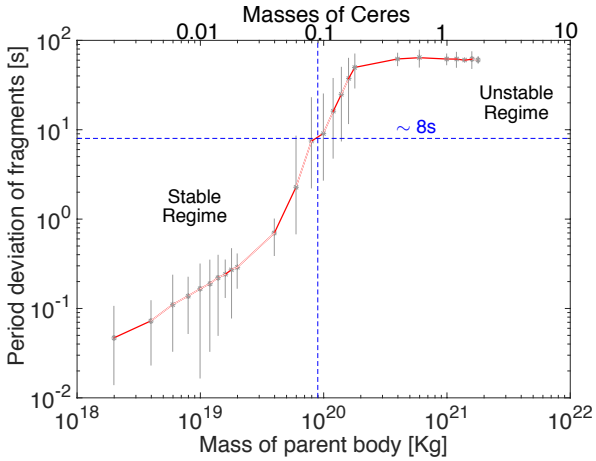

Figure 2. Mean of maximum fragment orbital period deviation, $\langle \Delta T_{\max} \rangle$ (see Section 4), for different parent body masses. Each point represents the mean of 100 simulations under the assumptions of completely circular orbits and fragment masses randomly ranging from 0.01% to 20% of the parent body's mass. Each simulation spans 5 years ($\simeq$ 9750 fragment's orbital cycles) .Blue dashed lines are the theoretical prediction for the mass of the parent body (Rappaport et al. 2016) and the maximum difference between the observed orbital periods and their mean (Gänsicke et al. 2016). Only low-mass systems tent to exhibit small interactions and orbital stability over time.

increase provides a robust upper limit the parent body's mass, which is close to one tenth of the mass of Ceres, and agrees well with the estimate of the parent body mass analytically derived by Rappaport et al. (2016).

5 ECCENTRICITY CONSTRAINTS

As well as mass, eccentricity is very likely to play an important role in the stability of the system. We therefore ran simulations modifying not only mass but also the eccentricity of the parent body.

By keeping track of $\Delta T_{\max}$ in the same way as outlined in Section 4, we increased the parent body's mass from $\sim 10^{18}$ kg to $\sim 10^{21}$ kg and its eccentricity from 10^{-3} to 10^{-1}. To obtain a $\langle \Delta T_{\max} \rangle$ we averaged over 50 two-year simulations per each pair of mass and eccentricity, henceforth denoted (M, e) pair.

Figure 3 exhibits contours which display $\langle \Delta T_{\max} \rangle$ as a function of mass and eccentricity of the parent body. A clear dependence on eccentricity can be seen, demonstrating that, (i) as well as mass, eccentricity plays a key role in period deviation, and (ii) that only systems with low mass and eccentricity exhibit small period deviations.

Low period deviations agree with observations, therefore, the area of greatest interest of Figure 3 is the lower-left corner. Consequently, we performed extra simulations to analyse in more detail the region from 2×10^{18} kg to 2×10^{19} kg and sampled eccentricities in the range 10^{-4} to 10^{-1}. We introduced the concept of "stable systems" to be able to study in detail those configurations that remain largely unperturbed over the entire time span of the simulation. We define a system as stable if none of the fragments collides with either the parent body or the star. With this definition, we run simulations until exactly 50 remain stable per (M, e) pair. We kept track of the number of unstable simulations to be able to define the fraction of

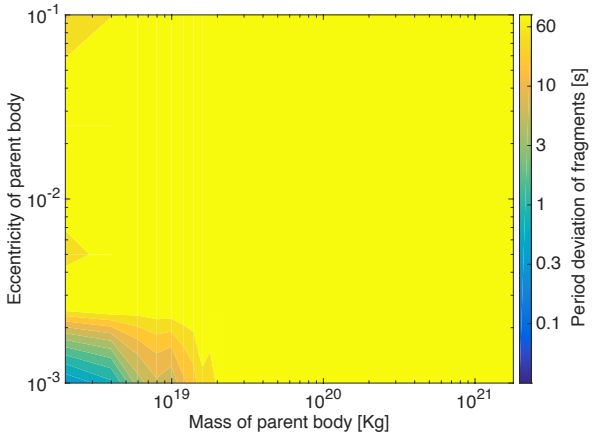

Figure 3. Mean of maximum fragment orbital period deviation, $\langle \Delta T_{\rm max} \rangle$ (see Section 4), as a function of the parent body's mass and eccentricity. Eccentricity and mass are sampled by 20 and 15 values, respectively, which are logarithmically spaced, and the fragment masses are randomly drawn ranging from 0.01% to 20% of the parent body's mass. Each (M, e) pair represents the mean of 50, 2-year simulations. Low values of $\langle \Delta T_{\rm max} \rangle$ are only found for both low parent body masses and low eccentricity.

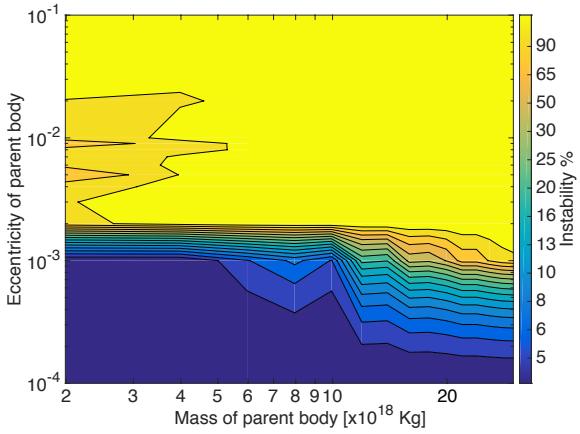

Figure 4. The fraction of unstable systems is defined as the ratio of 50 stable simulations over the total number of simulations performed (see Section 5), and it is shown as function of the parent body's mass and eccentricity. Stable systems are defined as systems without collisions between fragments and parent or the star. There is a clear increase in the number of unstable systems with larger eccentricities.

unstable systems per (M, e) pair, defined as the ratio of unstable simulations ($N_{\rm unstable}$) divided by the total number of simulations performed ($N_{\rm unstable} + 50$).

Figure 4 plots the fraction of unstable systems as a contour plot. A clear positive correlation can be seen between fraction of unstable systems and eccentricity, with a sharp increase in instability for eccentricities greater than 10^{-3}. Mass has a less drastic effect but also increases instability, more evidently for masses greater than 10^{19} kg.

Figure 5 plots $\langle \Delta T_{\rm max} \rangle$ of the 50 stable solutions found per (M, e) pair, both on linear and logarithmic eccentricity scales. A comparison between Figures 4 and 5 highlights how highly unstable regions (*i.e.* larger eccentricities) can still host systems with low

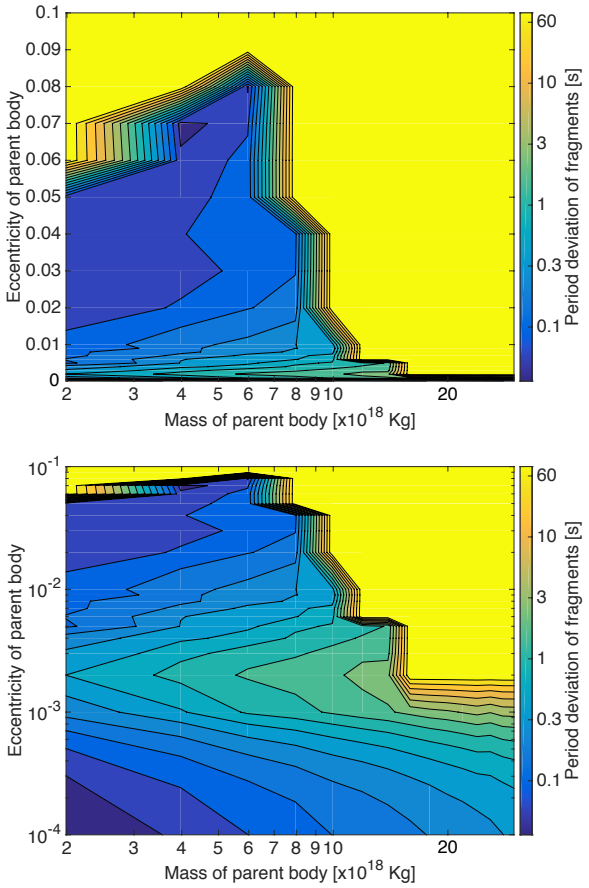

Figure 5. Mean of maximum fragment orbital period deviation, $\langle \Delta T_{\rm max} \rangle$ (see Section 4), averaged for 50 stable simulations per (M, e) pair (see Section 5), shown on a linear scale in the top panel and on a logarithmic scale below. While systems with high eccentricities of up to $\simeq 0.1$ are rarely stable (Fig. 4), they can have low $\langle \Delta T_{\rm max} \rangle$.

$\Delta T_{\rm max}$ – however, at a much reduced likelihood. The bottom panel of Figure 5 emphasizes the mass dependence of $\langle \Delta T_{\rm max} \rangle$ even for stable scenarios. Stable systems with masses higher than 10^{19}kg exhibit high perturbations which most probably will lead to collisions in the future. Alternatively, eccentricity does not show a prominent effect on stable, low-mass ($< 10^{19}$kg) systems.

Figure 6 displays the temporal evolution of stable systems. We computed not only $\langle \Delta T_{\rm max} \rangle$ but also Max$(\Delta T_{\rm max})$ and Min$(\Delta T_{\rm max})$, being the maximum and minimum of $\Delta T_{\rm max}$ recorded in the 50 stable simulations. Max$(\Delta T_{\rm max})$, $\langle \Delta T_{\rm max} \rangle$ and Min$(\Delta T_{\rm max})$ are plotted at three different epochs throughout the simulations, six months, one year and two years after the start of the simulation. Figure 6 reveals that there is not a noticeable variation of either Max$(\Delta T_{\rm max})$, $\langle \Delta T_{\rm max} \rangle$ or Min$(\Delta T_{\rm max})$ over time, meaning that stable systems do not evolve strongly with time and are robust regardless of sampling time. This finding is important because it ensures compatibility, and permits direct comparisons, between simulations that last years and observational data that only spans months.

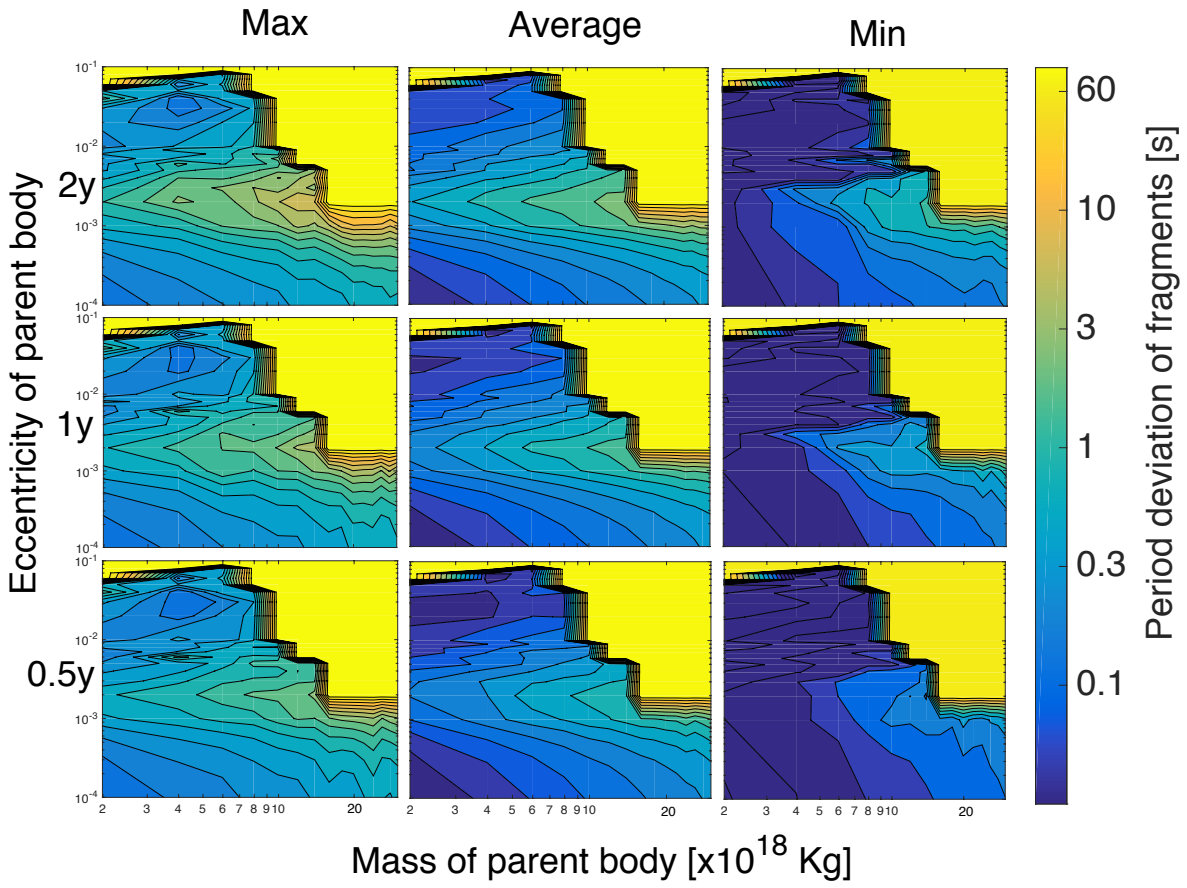

Figure 6. Max($\Delta T_{\rm max}$), $\langle \Delta T_{\rm max} \rangle$ and Min($\Delta T_{\rm max}$) for 50 stable simulations (see Section 5), as a function of the parent body's mass and eccentricity. All plots are repeated for three different epochs throughout the simulations: six months, one year and two years after the start of the simulation. The number of analysed values as well as assumptions are the same than in Figure 3. This figure illustrates the long-term robustness of stable systems over extended periods of time.

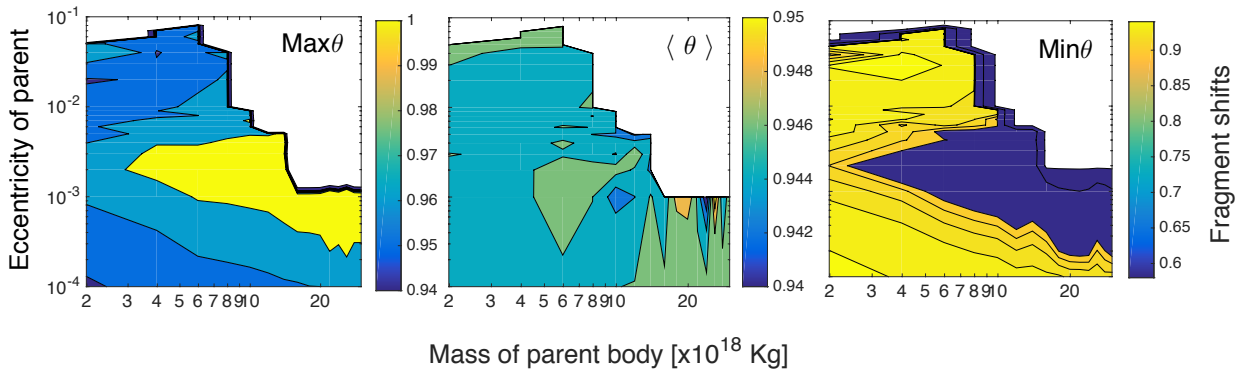

Figure 7. Max(θ), $\langle \theta \rangle$ and Min(θ) phase shifts in orbital cycles after 80 days (see Section 6) for 50 stable simulations, with respect to mass and eccentricity of the parent body. Max(θ) and Min(θ) show the same structure as Figure 5, while $\langle \theta \rangle$ remains almost constant regardless of mass or eccentricity, meaning that on average, all fragments shift on phase in a similar way.

6 PHASE SHIFTS

The fact that the parent body and the fragments have different orbital periods offers the possibility to determine phase shifts between them. By folding the transit signals of the fragments onto the parent's period, Rappaport et al. (2016) illustrated how the phase of the transit features shifts from night to night. Because $\Delta T_{\rm max}$ of stable systems remains almost constant in time, we used the stable simulations of Section 5 to calculate these phase shifts and obtain a direct comparison between observational data and our simulations.

In order to determine an average phase shift, $\langle \theta \rangle$, we computed the ratio between the period of each fragment and the parent's one, $\theta = T_{\rm frag}/T_{\rm parent}$, at each time step of the simulation (*i.e.*

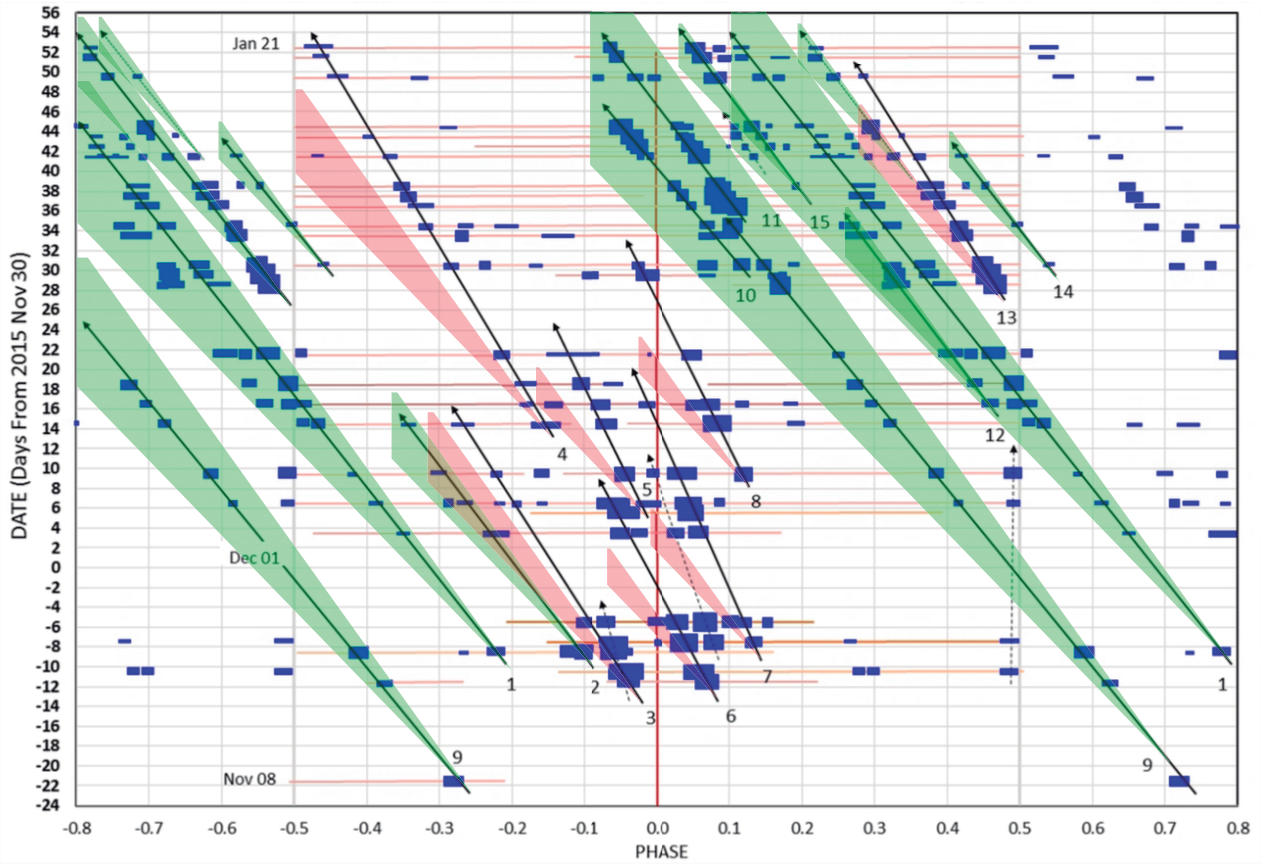

Figure 8. Superposition of Figure 6 of (Rappaport et al. 2016) and the ranges of phase shifts predicted by our simulations, confined by $\langle \mathrm{Max}(\theta) \rangle$ and $\langle \mathrm{Min}(\theta) \rangle$ (see Section 6). Expected ranges are shaded green if the observational prediction (Rappaport et al. 2016) fits with our simulations and red if it does not. Generally, computer predicted phase shifts suit observational data and every shaded range contains at least two linkable transits.

approximately 10 times per orbit). We averaged the shift over time and obtained a mean shift per orbit of the parent body, which can be transformed into mean phase shift per day or, to ease direct comparison with observational data, mean phase shift after 80 days, $\langle \theta \rangle$. We also kept the maximum and a minimum phase shift after 80 days, $\mathrm{Max}(\theta)$ and $\mathrm{Min}(\theta)$.We double-checked our results by first averaging the period and then calculating phase shifts, which lead to very similar results, never differing more than 5%.

Figure 7 shows $\mathrm{Max}(\theta)$, $\langle \theta \rangle$ and $\mathrm{Min}(\theta)$ as a function of the eccentricity and mass of the parent body. We obviated phase shifts for systems exhibiting high $\langle \Delta T_{\mathrm{max}} \rangle$ (yellow area on Figure 4) because observations suggest low period perturbations. Minimum and maximum phase shifts share a similar structure that resembles that of Figure 5. Mean phase shifts remain almost constant for all values of mass and eccentricity, meaning that on average, fragments tend to drift systematically regardless of their mass or eccentricity.

We averaged over all values of $\mathrm{Max}(\theta)$ and $\mathrm{Min}(\theta)$ shown in Figure 7 and obtained $\langle \mathrm{Max}(\theta) \rangle = 0.9941$ and $\langle \mathrm{Min}(\theta) \rangle = 0.8885$. We expect that most fragments experience phase shifts with respect to the parent that are contained between $\langle \mathrm{Max}(\theta) \rangle$ and $\langle \mathrm{Min}(\theta) \rangle$.

We superpose the range of phase shifts predicted by our simulations with the observations of Rappaport et al. (2016). Fragments identified by Rappaport et al. (2016) that fall within the expected range are shaded in green, those that fall outside the predicted range are shaded in red. Overall, the agreement is remarkably good. We note that some of the transits interpreted by Rappaport et al. (2016) as a single fragment fall outside the predicted range of phase shifts (*e.g.* #3–8), which illustrates both the difficulty in identifying individual fragments from the ever changing transits, and the possibility of additional dynamical processes among the fragments.

7 DISCUSSION

Constraining the mass of disintegrating objects orbiting a polluted white dwarf provides insights into the planetary system and the star itself. Asteroids have long since assumed to be source of the pollution (Graham et al. 1990; Jura 2003; Bear & Soker 2013), having been perturbed into the white dwarf disruption radius by external agents such as planets (Bonsor et al. 2011; Debes et al. 2012b; Frewen & Hansen 2014b; Veras et al. 2016b), moons (Payne et al. 016a,b), comets (Alcock et al. 1986; Veras et al. 2014b; Stone et al. 2015) and/or wide binary companions (Bonsor & Veras 2015). However, the size and mass distributions of the perturbed objects has remained unknown. Although WD 1145+017 provides a bound at just one snapshot in time, this singular constraint provides an anchor for future estimates and studies.

Perhaps more revealing is the relation between the orbiting mass and the convection zone mass of the parent star. Because WD 1145+017 is a metal-polluted helium-rich DBZ white dwarf, its atmosphere effectively keeps a record of all accreted material over the last Myr or so (e.g. Farihi et al. 2010; Girven et al. 2012;

Xu & Jura 2012). All this material may arise from the accretion of a single object, or multiple objects. The measured convection zone masses in DBZ white dwarfs range from about 10^{16} kg to 10^{23} kg, which roughly encompasses the mass range of Saturn's moon Phobos to Jupiter's moon Europa. The maximum mass of the objects orbiting WD 1145+017 ($\sim 10^{21}$ kg) towards the upper end of this range (see Fig. 6 of Veras 2016).

8 CONCLUSIONS

Despite many on-going observations of WD 1145+017, it has not been possible to robustly constrain the mass and eccentricity of the orbiting debris. We have performed N-body simulations to gain insight on such uncertainties and revealed that either masses greater than $\simeq 10^{20}$ kg (0.1 the mass of Ceres) or orbits that are not nearly circular (eccentricity $> 10^{-3}$) increase the likelihood of dynamical instability during the timespan of the observations. We also computed an expected phase shift for the orbiting bodies, which allowed us to validate most of the objects detected by Rappaport et al. (2016).

Future work could include a disruption model for the disintegrating bodies. This model might help better pinpoint the disruption radius of WD 1145+017 as well as understand poorly-known processes such as the disruption and accretion of planetesimals in main-sequence planetary systems (Rappaport et al. 2012; Croll et al. 2014; Rappaport et al. 2014; Bochinski et al. 2015; Sanchis-Ojeda et al. 2015).

ACKNOWLEDGMENTS

The undergraduate exchange program of Engineering Physics from UPC (BarcelonaTech) made this research possible.

DV and BTG have received funding from the European Research Council under the European Union's Seventh Framework Programme (FP/2007-2013)/ERC Grant Agreement n. 320964 (WDTracer).

REFERENCES

Alcock C., Fristrom C. C., Siegelman R., 1986, ApJ, 302, 462
Alonso R., Rappaport S., Deeg H. J., Palle E., 2016, preprint, (arXiv:1603.08823)
Bear E., Soker N., 2013, New Astron., 19, 56
Berg C., Wegner G., Foltz C. B., Chaffee Jr. F. H., Hewett P. C., 1992, ApJS, 78, 409
Bergfors C., Farihi J., Dufour P., Rocchetto M., 2014, MNRAS, 444, 2147
Bochinski J. J., Haswell C. A., Marsh T. R., Dhillon V. S., Littlefair S. P., 2015, ApJ, 800, L21
Bonsor A., Veras D., 2015, MNRAS, 454, 53
Bonsor A., Mustill A. J., Wyatt M. C., 2011, MNRAS, 414, 930
Burleigh M. R., Clarke F. J., Hodgkin S. T., 2002, MNRAS, 331, L41
Carter-Bond J. C., O'Brien D. P., Raymond S. N., 2012, ApJ, 760, 44
Chambers J. E., 1999, MNRAS, 304, 793
Croll B., et al., 2014, ApJ, 786, 100
Croll B., et al., 2015, preprint, (arXiv:1510.06434)
Debes J. H., Sigurdsson S., 2002, ApJ, 572, 556
Debes J. H., Walsh K. J., Stark C., 2012a, ApJ, 747, 148
Debes J. H., Walsh K. J., Stark C., 2012b, ApJ, 747, 148
Debes J. H., Kilic M., Faedi F., Shkolnik E. L., Lopez-Morales M., Weinberger A. J., Slesnick C., West R. G., 2012c, ApJ, 754, 59
Farihi J., 2016, New Astron. Rev., 71, 9
Farihi J., Jura M., Zuckerman B., 2009, ApJ, 694, 805
Farihi J., Barstow M. A., Redfield S., Dufour P., Hambly N. C., 2010, MNRAS, 404, 2123
Frewen S. F. N., Hansen B. M. S., 2014a, MNRAS, 439, 2442
Frewen S. F. N., Hansen B. M. S., 2014b, MNRAS, 439, 2442
Friedrich S., Koester D., Christlieb N., Reimers D., Wisotzki L., 2000, A&A, 363, 1040
Gänsicke B. T., Marsh T. R., Southworth J., Rebassa-Mansergas A., 2006, Science, 314, 1908
Gänsicke B. T., Koester D., Farihi J., Girven J., Parsons S. G., Breedt E., 2012, MNRAS, 424, 333
Gänsicke B. T., et al., 2016, ApJ, 818, L7
Girven J., Brinkworth C. S., Farihi J., Gänsicke B. T., Hoard D. W., Marsh T. R., Koester D., 2012, ApJ, 749, 154
Graham J. R., Matthews K., Neugebauer G., Soifer B. T., 1990, ApJ, 357, 216
Jura M., 2003, ApJ, 584, L91
Kilic M., von Hippel T., Leggett S. K., Winget D. E., 2006, ApJ, 646, 474
Koester D., Gänsicke B. T., Farihi J., 2014, A&A, 566, A34
Mustill A. J., Villaver E., 2012, ApJ, 761, 121
Payne M. J., Veras D., Holman M. J., Gänsicke B. T., 2016, MNRAS, 457, 217
Payne M. J., Veras D., Holman M. J., Gänsicke B. T., 2016a, MNRAS, 457, 217
Payne M. J., Veras D., Gänsicke B. T., Holman M. J., 2016b, Submitted to MNRAS
Rappaport S., et al., 2012, ApJ, 752, 1
Rappaport S., Barclay T., DeVore J., Rowe J., Sanchis-Ojeda R., Still M., 2014, ApJ, 784, 40
Rappaport S., Gary B. L., Kaye T., Vanderburg A., Croll B., Benni P., Foote J., 2016, preprint, (arXiv:1602.00740)
Sanchis-Ojeda R., et al., 2015, ApJ, 812, 112
Stone N., Metzger B. D., Loeb A., 2015, MNRAS, 448, 188
Vanderburg A., et al., 2015, Nature, 526, 546
Veras D., 2016, Royal Society Open Science, 3, 150571
Veras D., Mustill A. J., Bonsor A., Wyatt M. C., 2013, MNRAS, 431, 1686
Veras D., Leinhardt Z. M., Bonsor A., Gänsicke B. T., 2014a, MNRAS, 445, 2244
Veras D., Shannon A., Gänsicke B. T., 2014b, MNRAS, 445, 4175
Veras D., Eggl S., Gänsicke B. T., 2015a, MNRAS, 451, 2814
Veras D., Leinhardt Z. M., Eggl S., Gänsicke B. T., 2015b, MNRAS, 451, 3453
Veras D., Leinhardt Z. M., Eggl S., Gänsicke B. T., 2015c, MNRAS, 451, 3453
Veras D., Eggl S., Gänsicke B. T., 2015d, MNRAS, 452, 1945
Veras D., Marsh T. M., Gänsicke B. T., 2016a, Submitted to MNRAS
Veras D., Mustill A. J., Gänsicke B. T., Redfield S., Georgakarakos N., Bowler A. B., Lloyd M. J. S., 2016b, MNRAS, 458, 3942
Villaver E., Livio M., 2007, ApJ, 661, 1192
Xu S., Jura M., 2012, ApJ, 745, 88
Xu S., Jura M., Koester D., Klein B., Zuckerman B., 2014, ApJ, 783, 79
Xu S., Jura M., Dufour P., Zuckerman B., 2016, ApJ, 816, L22
Zhou G., et al., 2016, preprint, (arXiv:1604.07405)
Zuckerman B., Becklin E. E., 1987, Nature, 330, 138
Zuckerman B., Koester D., Reid I. N., Hünsch M., 2003, ApJ, 596, 477
Zuckerman B., Koester D., Melis C., Hansen B. M., Jura M., 2007, ApJ, 671, 872
Zuckerman B., Melis C., Klein B., Koester D., Jura M., 2010, ApJ, 722, 725

8

Conclusions

In this work we review the essentials for a basic understanding of the WD 1145+017 system, which offers for the first time a unique opportunity to validate a tidal disruption model that has long been theorised. While WD 1145+017 system has been subject to a number of detailed observational follow-up studies, relatively little is known about its disintegrating planetary system. By taking a different and complementary approach, we performed numerical simulations with the aim to alleviate the dearth of constraints defining WD 1145+017's orbiting bodies.

Using N-body simulations we have been able to recreate the temporal evolution of the system and reproduce the interactions between the orbiting bodies. By keeping track of the orbital period, we have constrained under which circumstances our simulations most resemble the reality. We presented that debris with large masses ($m > \sim 10^{20}$ kg) or eccentricities ($e > \sim 10^{-3}$) cause long-term dynamical instabilities that would counter observations. We also provided a direct comparison between our simulations and observations by recreating phase shifts between debris, which have been a major source of observational information for the system.

Although this work specially focuses on WD 1145+017, it may provide a first estimate for future studies on disintegrating objects orbiting a white dwarf. The obtained mass and eccentricity constraints help to better estimate the disruption radius of a star, provide an order-of-magnitude approximation for disk properties and better understand processes such as disintegration, orbital circularisation and the actual nature of those orbiting bodies.

Despite the insight provided by this work, there is still much room for new research on the system. New simulations could include tidal disruption models, interaction with the dusty and gaseous disk or a better model of the white dwarf. Additionally, numerical model's precision will improve when more observations are available. In preparation, we have already started to study new light-curves to better understand the system and the processes behind it.

Bibliography

[1] L. G. Althaus, A. H. Córsico, J. Isern, and E. García-Berro. Evolutionary and pulsational properties of white dwarf stars. *Astronomy and Astrophysics Reviews*, 18:471–566, October 2010. http://adsabs.harvard.edu/abs/2010A%26ARv..18..471A.

[2] D. Koester. *White Dwarf Stars*, page 559. 2013. http://adsabs.harvard.edu/abs/2013pss4.book..559K.

[3] M. A. Wood. Astero-Archaeology: Reading the Galactic History Recorded in the White Dwarf Stars. *Publications of the ASP*, 102:954, August 1990. http://adsabs.harvard.edu/abs/1990PASP..102..954W.

[4] H. N. Russell. Relations Between the Spectra and Other Characteristics of the Stars. *Popular Astronomy*, 22:331–351, June 1914. http://adsabs.harvard.edu/abs/1914PA....22..331R.

[5] W. S. Adams. An A-Type Star of Very Low Luminosity. *Publications of the ASP*, 26:198, October 1914. http://adsabs.harvard.edu/abs/1914PASP...26..198A.

[6] W. S. Adams. The Spectrum of the Companion of Sirius. *Publications of the ASP*, 27:236, December 1915. http://adsabs.harvard.edu/abs/1915PASP...27..236A.

[7] W. S. Adams. The relativity displacement of the spectral lines in the companion of Sirius. *The Observatory*, 48:337–342, November 1925. http://adsabs.harvard.edu/abs/1925Obs....48..337A.

[8] H. N. Russell. REVIEW: The Internal Constitution of the Stars by A. S. Eddington. *Astrophysical Journal*, 67:83, January 1928. http://adsabs.harvard.edu/abs/1928ApJ....67...83R.

[9] R. H. Fowler. On dense matter. *Monthly Notices of the RAS*, 87:114–122, December 1926. http://adsabs.harvard.edu/abs/1926MNRAS..87..114F.

[10] P. A. M. Dirac. On the Theory of Quantum Mechanics. *Proceedings of the Royal Society of London Series A*, 112:661–677, October 1926. http://adsabs.harvard.edu/abs/1926RSPSA.112..661D.

[11] W. Anderson. Gewöhnliche Materie und strahlende Energie als verschiedene #8222Phasen“ eines und desselben Grundstoffes. *Zeitschrift fur Physik*, 54:433–444, May 1929. http://adsabs.harvard.edu/abs/1929ZPhy...54..433A.

[12] E. Stoner. The Equilibrium of Dense Stars. *The London, Edinburgh, and Dublin Philosophical Magazine and Journal of Science: Series 7, Volume 9, Issue 60, p. 944-963*, 9:944–963, January 1930. http://adsabs.harvard.edu/abs/1930LEDPM...9..944S.

[13] S. Chandrasekhar. The Maximum Mass of Ideal White Dwarfs. *Astrophysical Journal*,

74:81, July 1931. http://adsabs.harvard.edu/abs/1931ApJ....74...81C.

[14] S. Chandrasekhar. *An introduction to the study of stellar structure*. 1939. http://adsabs.harvard.edu/abs/1939isss.book.....C.

[15] D. D. Clayton. *Principles of stellar evolution and nucleosynthesis*. 1968. http://adsabs.harvard.edu/abs/1968psen.book.....C.

[16] J. B. Holberg. How Degenerate Stars Came to be Known as White Dwarfs. In *American Astronomical Society Meeting Abstracts*, volume 37 of *Bulletin of the American Astronomical Society*, page 1503, December 2005. http://adsabs.harvard.edu/abs/2005AAS...20720501H.

[17] J. H. Jeans. The Stability of a Spherical Nebula. *Philosophical Transactions of the Royal Society of London Series A*, 199:1–53, 1902. http://adsabs.harvard.edu/abs/1902RSPTA.199....1J.

[18] E. Hertzsprung. Über die photographische Schwärzungskurve. *Astronomische Nachrichten*, 190:119, December 1911. http://adsabs.harvard.edu/abs/1911AN....190..119H.

[19] E. Garcia-Berro, M. Hernanz, J. Isern, and R. Mochkovitch. Properties of high-density binary mixtures and the age of the universe from white dwarf stars. *Nature*, 333:642–644, June 1988. http://adsabs.harvard.edu/abs/1988Natur.333..642G.

[20] D. E. Winget, C. J. Hansen, J. Liebert, H. M. van Horn, G. Fontaine, R. E. Nather, S. O. Kepler, and D. Q. Lamb. An independent method for determining the age of the universe. *Astrophysical Journal*, 315:L77–L81, April 1987. http://adsabs.harvard.edu/abs/1987ApJ...315L..77W.

[21] H. A. Bethe. Energy Production in Stars. *Physical Review*, 55:434–456, March 1939. http://adsabs.harvard.edu/abs/1939PhRv...55..434B.

[22] W. A. Fowler. Experimental and theoretical nuclear astrophysics: the quest for the origin of the elements. *Reviews of Modern Physics*, 56:149–179, April 1984. http://adsabs.harvard.edu/abs/1984RvMP...56..149F.

[23] D. Koester, H. Schulz, and V. Weidemann. Atmospheric parameters and mass distribution of DA white dwarfs. *Astronomy and Astrophysics*, 76:262–275, July 1979. http://adsabs.harvard.edu/abs/1979A%26A....76..262K.

[24] E. M. Sion, J. L. Greenstein, J. D. Landstreet, J. Liebert, H. L. Shipman, and G. A. Wegner. A proposed new white dwarf spectral classification system. *Astrophysical Journal*, 269:253–257, June 1983. http://adsabs.harvard.edu/abs/1983ApJ...269..253S.

[25] A. Renzini. Mass loss and stellar evolution. In B. E. Westerlund, editor, *Stars and star systems*, volume 75 of *Astrophysics and Space Science Library*, pages 155–171, 1979. http://adsabs.harvard.edu/abs/1979ASSL...75..155R.

[26] T. Blöcker. Evolution on the AGB and beyond: on the formation of H-deficient post-AGB stars. *Astrophysics and Space Science*, 275:1–14, January 2001. http://adsabs.harvard.edu/abs/2001Ap%26SS.275....1B.

[27] J. L. Greenstein. Spectrophotometry of the white dwarfs. *Astrophysical Journal*, 276:602–620, January 1984. http://adsabs.harvard.edu/abs/1984ApJ...276..602G.

[28] G. Fontaine and F. Wesemael. Recent advances in the theory of white dwarf spectral evolution. In A. G. D. Philip, D. S. Hayes, and J. W. Liebert, editors, *IAU Colloq. 95: Second Conference on Faint Blue Stars*, pages 319–326, 1987. http://adsabs.harvard.edu/abs/1987fbs..conf..319F.

[29] S. Friedrich, D. Koester, N. Christlieb, D. Reimers, and L. Wisotzki. Cool helium-rich white dwarfs from the Hamburg/ESO survey. *Astronomy and Astrophysics*, 363:1040–1050, November 2000. http://adsabs.harvard.edu/abs/2000A%26A...363.1040F.

[30] L. Mestel. On the theory of white dwarf stars. I. The energy sources of white dwarfs. *Monthly Notices of the RAS*, 112:583, 1952. http://adsabs.harvard.edu/abs/1952MNRAS.112..583M.

[31] G. Beaudet, V. Petrosian, and E. E. Salpeter. Energy Losses due to Neutrino Processes. *Astrophysical Journal*, 150:979, December 1967. http://adsabs.harvard.edu/abs/1967ApJ...150..979B.

[32] I. Renedo, L. G. Althaus, M. M. Miller Bertolami, A. D. Romero, A. H. Córsico, R. D. Rohrmann, and E. García-Berro. New Cooling Sequences for Old White Dwarfs. *Astrophysical Journal*, 717:183–195, July 2010. http://adsabs.harvard.edu/abs/2010ApJ...717..183R.

[33] I. Kant. *Universal natural history and theory of the heavens*. Ann Arbor paperbacks. University of Michigan Press, 1969. https://books.google.co.uk/books?id=HvPWAAAAMAAJ.

[34] P.S. de Laplace. *Exposition du système du monde*. Courcier, 1808. https://books.google.co.uk/books?id=JTEAAAAAQAAJ.

[35] R.P. Miller. *René Descartes: Principles of Philosophy: Translated, with Explanatory Notes*. Synthese Historical Library. Springer Netherlands, 1984. https://books.google.co.uk/books?id=8vt0uWWVzEYC.

[36] C. F. V. Weizsäcker. Über die Entstehung des Planetensystems. Mit 2 Abbildungen. *Zeitschrift fuer Astrophysik*, 22:319, 1944. http://adsabs.harvard.edu/abs/1943ZA....22..319W.

[37] G. P. Kuiper. On the Evolution of the Protoplanets. *Proceedings of the National Academy of Science*, 37:383–393, July 1951. http://adsabs.harvard.edu/abs/1951PNAS...37..383K.

[38] A. G. W. Cameron. Physical Conditions in the Primitive Solar Nebula. In P. M. Millman, editor, *Meteorite Research*, volume 12 of *Astrophysics and Space Science Library*, page 7, 1969.

[39] F. Hoyle. The Origin of the Solar Nebula. *Quarterly Journal of the RAS*, 1:28, September 1960. http://adsabs.harvard.edu/abs/1960QJRAS...1...28H.

[40] F. Shu, J. Najita, E. Ostriker, F. Wilkin, S. Ruden, and S. Lizano. Magnetocentrifugally driven flows from young stars and disks. 1: A generalized model. *Astrophysical Journal*, 429:781–796, July 1994. http://adsabs.harvard.edu/abs/1994ApJ...429..781S.

[41] P. Barge and J. Sommeria. Did planet formation begin inside persistent gaseous vortices? *Astronomy and Astrophysics*, 295:L1–L4, March 1995. http://adsabs.harvard.edu/abs/1995A%26A...295L...1B.

[42] H. H. Klahr and P. Bodenheimer. Turbulence in Accretion Disks: Vorticity Generation and Angular Momentum Transport via the Global Baroclinic Instability. *Astrophysical Journal*, 582:869–892, January 2003. http://adsabs.harvard.edu/abs/2003ApJ...582..869K.

[43] P.J. Armitage. *Astrophysics of Planet Formation*. Cambridge University Press, 2010. https://books.google.co.uk/books?id=zjlZQnFfMs8C.

[44] H. Klahr and W. Brandner. *Planet Formation: Theory, Observations, and Experiments*. Cambridge Astrobiology. Cambridge University Press, 2006. https://books.google.co.uk/books?id=_37CR1DfPUcC.

[45] V. S. Safronov. *Evoliutsiia doplanetnogo oblaka.* 1969. http://adsabs.harvard.edu/abs/1969edo..book.....S.

[46] K. E. Haisch, Jr., E. A. Lada, and C. J. Lada. Disk Frequencies and Lifetimes in Young Clusters. *The Astrophysical Journal*, 553:L153–L156, June 2001. http://adsabs.harvard.edu/abs/2001ApJ...553L.153H.

[47] C. P. Dullemond and C. Dominik. Dust coagulation in protoplanetary disks: A rapid depletion of small grains. *Astronomy and Astrophysics*, 434:971–986, May 2005. http://adsabs.harvard.edu/abs/2005A%26A...434..971D.

[48] E. W. Thommes, M. J. Duncan, and H. F. Levison. Oligarchic growth of giant planets. *Icarus*, 161:431–455, February 2003. http://adsabs.harvard.edu/abs/2003Icar..161..431T.

[49] E. Chiang and A. N. Youdin. Forming Planetesimals in Solar and Extrasolar Nebulae. *Annual Review of Earth and Planetary Sciences*, 38:493–522, May 2010. http://adsabs.harvard.edu/abs/2010AREPS..38..493C.

[50] I. Adachi, C. Hayashi, and K. Nakazawa. The gas drag effect on the elliptical motion of a solid body in the primordial solar nebula. *Progress of Theoretical Physics*, 56:1756–1771, December 1976. http://adsabs.harvard.edu/abs/1976PThPh..56.1756A.

[51] F. Perri and A. G. W. Cameron. Hydrodynamic instability of the solar nebula in the presence of a planetary core. *Icarus*, 22:416–425, August 1974. http://adsabs.harvard.edu/abs/1974Icar...22..416P.

[52] A. P. Boss. Formation of giant gaseous protoplanets by gravitational instability. In *Lunar and Planetary Science Conference*, volume 28 of *Lunar and Planetary Science Conference*, page 137, March 1997. http://adsabs.harvard.edu/abs/1997LPI....28..137B.

[53] A. Wolszczan and D. A. Frail. A planetary system around the millisecond pulsar PSR1257 + 12. *Nature*, 355:145–147, January 1992. http://adsabs.harvard.edu/abs/1992Natur.355..145W.

[54] M. Mayor and D. Queloz. A Jupiter-mass companion to a solar-type star. *Nature*, 378:355–359, November 1995. http://adsabs.harvard.edu/abs/1995Natur.378..355M.

[55] O. Struve. Proposal for a project of high-precision stellar radial velocity work. *The Observatory*, 72:199–200, October 1952. http://adsabs.harvard.edu/abs/1952Obs...72..199S.

[56] A. Vanderburg, J. A. Johnson, S. Rappaport, A. Bieryla, J. Irwin, J. A. Lewis,

D. Kipping, W. R. Brown, P. Dufour, D. R. Ciardi, R. Angus, L. Schaefer, D. W. Latham, D. Charbonneau, C. Beichman, J. Eastman, N. McCrady, R. A. Wittenmyer, and J. T. Wright. A disintegrating minor planet transiting a white dwarf. *Nature*, 526:546–549, October 2015. http://adsabs.harvard.edu/abs/2015Natur.526..546V.

[57] B. T. Gänsicke, A. Aungwerojwit, T. R. Marsh, V. S. Dhillon, D. I. Sahman, D. Veras, J. Farihi, P. Chote, R. Ashley, S. Arjyotha, S. Rattanasoon, S. P. Littlefair, D. Pollacco, and M. R. Burleigh. High-speed Photometry of the Disintegrating Planetesimals at WD1145+017: Evidence for Rapid Dynamical Evolution. *The Astrophysical Journal Letters*, 818:L7, February 2016. http://adsabs.harvard.edu/abs/2016ApJ...818L...7G.

[58] M. Perryman. *The Exoplanet Handbook*. Cambridge University Press, 2011. https://books.google.nl/books?id=xekY6FuKuAcC.

[59] V. Mannings, A. Boss, and S.S. Russell. *Protostars and Planets IV*. Number v. 4 in Space science series. University of Arizona Press, 2000. https://books.google.nl/books?id=o4_vAAAAMAAJ.

[60] I.-J. Sackmann, A. I. Boothroyd, and K. E. Kraemer. Our Sun. III. Present and Future. *Astrophysical Journal*, 418:457, November 1993. http://adsabs.harvard.edu/abs/1993ApJ...418..457S.

[61] F. A. Rasio, C. A. Tout, S. H. Lubow, and M. Livio. Tidal Decay of Close Planetary Orbits. *Astrophysical Journal*, 470:1187, October 1996. http://adsabs.harvard.edu/abs/1996ApJ...470.1187R.

[62] K.-P. Schröder and R. Connon Smith. Distant future of the Sun and Earth revisited. *Monthly Notices of the RAS*, 386:155–163, May 2008. http://adsabs.harvard.edu/abs/2008MNRAS.386..155S.

[63] M. J. Duncan and J. J. Lissauer. The Effects of Post-Main-Sequence Solar Mass Loss on the Stability of Our Planetary System. *Icarus*, 134:303–310, August 1998. http://adsabs.harvard.edu/abs/1998Icar..134..303D.

[64] J. H. Debes and S. Sigurdsson. Are There Unstable Planetary Systems around White Dwarfs? *Astrophysical Journal*, 572:556–565, June 2002. http.

[65] A. Bonsor, A. J. Mustill, and M. C. Wyatt. Dynamical effects of stellar mass-loss on a Kuiper-like belt. *Monthly Notices of the RAS*, 414:930–939, June 2011. http://adsabs.harvard.edu/abs/2011MNRAS.414..930B.

[66] Dimitri Veras. Post-main-sequence planetary system evolution. *Royal Society Open Science*, 3(2), 2016. http://rsos.royalsocietypublishing.org/content/3/2/150571.

[67] J. Farihi. Circumstellar debris and pollution at white dwarf stars. *New Astronomy Reviews*, 71:9–34, April 2016. http://adsabs.harvard.edu/abs/2016NewAR..71....9F.

[68] S. J. Kenyon and L. Hartmann. Pre-Main-Sequence Evolution in the Taurus-Auriga Molecular Cloud. *Astrophysical Journal*, 101:117, November 1995. http://adsabs.harvard.edu/abs/1995ApJS..101..117K.

[69] B. Zuckerman, T. Forveille, and J. H. Kastner. Inhibition of giant-planet formation by rapid gas depletion around young stars. *Nature*, 373:494–496, February 1995. http://adsabs.harvard.edu/abs/1995Natur.373..494Z.

[70] B. T. Gänsicke, T. R. Marsh, J. Southworth, and A. Rebassa-Mansergas. A Gaseous Metal Disk Around a White Dwarf. *Science*, 314:1908, December 2006. http://adsabs.harvard.edu/abs/2006Sci...314.1908G.

[71] M. Jura. A Tidally Disrupted Asteroid around the White Dwarf G29-38. *Astrophysical Journal Letters*, 584:L91–L94, February 2003. http://adsabs.harvard.edu/abs/2003ApJ...584L..91J.

[72] R. G. Probst. Infrared Detection of Very Low Mass Stars. 1981. http://adsabs.harvard.edu/abs/1981PhDT.....45P.

[73] S. D. Barber, A. J. Patterson, M. Kilic, S. K. Leggett, P. Dufour, J. S. Bloom, and D. L. Starr. The Frequency of Debris Disks at White Dwarfs. *Astrophysical Journal*, 760:26, November 2012. http://adsabs.harvard.edu/abs/2012ApJ...760...26B.

[74] B. Zuckerman and E. E. Becklin. Excess infrared radiation from a white dwarf - an orbiting brown dwarf? *Nature*, 330:138–140, November 1987. http://adsabs.harvard.edu/abs/1987Natur.330..138Z.

[75] J. R. Graham, K. Matthews, G. Neugebauer, and B. T. Soifer. The infrared excess of G29-38 - A brown dwarf or dust? *Astrophysical Journal*, 357:216–223, July 1990. http://adsabs.harvard.edu/abs/1990ApJ...357..216G.

[76] M. Kilic, T. von Hippel, S. K. Leggett, and D. E. Winget. Excess Infrared Radiation from the Massive DAZ White Dwarf GD 362: A Debris Disk? *Astrophysical Journal*, 632:L115–L118, October 2005. http://adsabs.harvard.edu/abs/2005ApJ...632L.115K.

[77] E. E. Becklin, J. Farihi, M. Jura, I. Song, A. J. Weinberger, and B. Zuckerman. A Dusty Disk around GD 362, a White Dwarf with a Uniquely High Photospheric Metal Abundance. *The Astrophysical Journal*, 632:L119–L122, October 2005. http://adsabs.harvard.edu/abs/2005ApJ...632L.119B.

[78] G. Zhou, L. Kedziora-Chudczer, J. Bailey, J. P. Marshall, D. D. R. Bayliss, C. Stockade, P. Nelson, T. G. Tan, J. E. Rodriguez, C. G. Tinney, D. Dragomir, K. Colon, A. Shporer, J. Bento, R. Sefako, K. Horne, and W. Cochran. Simultaneous infrared and optical observations of the transiting debris cloud around WD 1145+017. *ArXiv e-prints*, April 2016. http://adsabs.harvard.edu/abs/2016arXiv160407405Z.

[79] S. Wolf, F. Malbet, R. Alexander, J.-P. Berger, M. Creech-Eakman, G. Duchêne, A. Dutrey, C. Mordasini, E. Pantin, F. Pont, J.-U. Pott, E. Tatulli, and L. Testi. Circumstellar disks and planets. Science cases for next-generation optical/infrared long-baseline interferometers. *Astronomy and Astrophysics Review manuscript*, 20:52, March 2012.

[80] E. Schatzman. Théorie du débit d'énergie des naines blanches. *Annales d'Astrophysique*, 8:143, January 1945. http://adsabs.harvard.edu/abs/1945AnAp...8..143S.

[81] J. Farihi, M. Jura, and B. Zuckerman. Infrared Signatures of Disrupted Minor Planets at White Dwarfs. *Astrophysical Journal*, 694:805–819, April 2009. http://adsabs.harvard.edu/abs/2009ApJ...694..805F.

[82] C. Bergfors, J. Farihi, P. Dufour, and M. Rocchetto. Signs of a faint disc population at polluted white dwarfs. *Monthly Notices of the RAS*, 444:2147–2156, November 2014. http://adsabs.harvard.edu/abs/2014MNRAS.444.2147B.

[83] S. Xu, M. Jura, P. Dufour, and B. Zuckerman. Evidence for Gas from a Disintegrating Extrasolar Asteroid. *The Astrophysical Journal Letters*, 816:L22, January 2016. http://adsabs.harvard.edu/abs/2016ApJ...816L..22X.

[84] M. Jura. Pollution of Single White Dwarfs by Accretion of Many Small Asteroids. *The Astronomical Journal*, 135:1785–1792, May 2008. http://adsabs.harvard.edu/abs/2008AJ....135.1785J.

[85] D. Veras, Z. M. Leinhardt, A. Bonsor, and B. T. Gänsicke. Formation of planetary debris discs around white dwarfs - I. Tidal disruption of an extremely eccentric asteroid. *Monthly Notices of the RAS*, 445:2244–2255, December 2014. http://adsabs.harvard.edu/abs/2014MNRAS.445.2244V.

[86] D. Veras. Post-main-sequence planetary system evolution. *Royal Society Open Science*, 3:150571, February 2016. http://adsabs.harvard.edu/abs/2016RSOS....3.0571V.

[87] B. Zuckerman, D. Koester, I. N. Reid, and M. Hünsch. Metal Lines in DA White Dwarfs. *Astrophysical Journal*, 596:477–495, October 2003. http://adsabs.harvard.edu/abs/2003ApJ...596..477Z.

[88] B. Zuckerman, C. Melis, B. Klein, D. Koester, and M. Jura. Ancient Planetary Systems are Orbiting a Large Fraction of White Dwarf Stars. *Astrophysical Journal*, 722:725–736, October 2010. http://adsabs.harvard.edu/abs/2010ApJ...722..725Z.

[89] D. Koester, J. Provencal, and B. T. Gänsicke. Atmospheric parameters and carbon abundance for hot DB white dwarfs. *Astronomy and Astrophysics*, 568:A118, August 2014.

[90] J. Dupuis, G. Fontaine, C. Pelletier, and F. Wesemael. A study of metal abundance patterns in cool white dwarfs. II - Simulations of accretion episodes. *Astrophysical Journal*, 84:73–89, January 1993. http://adsabs.harvard.edu/abs/1993ApJS...84...73D.

[91] M. Jura and E. D. Young. Extrasolar Cosmochemistry. *Annual Review of Earth and Planetary Sciences*, 42:45–67, May 2014. http://adsabs.harvard.edu/abs/2014AREPS..42...45J.

[92] A. Cassan, D. Kubas, J.-P. Beaulieu, M. Dominik, K. Horne, J. Greenhill, J. Wambsganss, J. Menzies, A. Williams, U. G. Jørgensen, A. Udalski, D. P. Bennett, M. D. Albrow, V. Batista, S. Brillant, J. A. R. Caldwell, A. Cole, C. Coutures, K. H. Cook, S. Dieters, D. D. Prester, J. Donatowicz, P. Fouqué, K. Hill, N. Kains, S. Kane, J.-B. Marquette, R. Martin, K. R. Pollard, K. C. Sahu, C. Vinter, D. Warren, B. Watson, M. Zub, T. Sumi, M. K. Szymański, M. Kubiak, R. Poleski, I. Soszynski, K. Ulaczyk, G. Pietrzyński, and Ł. Wyrzykowski. One or more bound planets per Milky Way star from microlensing observations. *Nature*, 481:167–169, January 2012. http://adsabs.harvard.edu/abs/2012Natur.481..167C.

[93] F. Fressin, G. Torres, D. Charbonneau, S. T. Bryson, J. Christiansen, C. D. Dressing, J. M. Jenkins, L. M. Walkowicz, and N. M. Batalha. The False Positive Rate of Kepler and the Occurrence of Planets. *Astrophysical Journal*, 766:81, April 2013. http://adsabs.harvard.edu/abs/2013ApJ...766...81F.

[94] A. J. Mustill and E. Villaver. Foretellings of Ragnarök: World-engulfing Asymptotic Giants and the Inheritance of White Dwarfs. *Astrophysical Journal*, 761:121, December 2012. http://adsabs.harvard.edu/abs/2012ApJ...761..121M.

[95] D. Veras, A. J. Mustill, A. Bonsor, and M. C. Wyatt. Simulations of two-planet systems through all phases of stellar evolution: implications for the instability boundary and white dwarf pollution. *Monthly Notices of the RAS*, 431:1686–1708, May 2013. http://adsabs.harvard.edu/abs/2013MNRAS.431.1686V.

[96] M. Kilic, T. von Hippel, S. K. Leggett, and D. E. Winget. Debris Disks around White Dwarfs: The DAZ Connection. *Astrophysical Journal*, 646:474–479, July 2006. http://adsabs.harvard.edu/abs/2006ApJ...646..474K.

[97] M. Rocchetto, J. Farihi, B. T. Gänsicke, and C. Bergfors. The frequency and infrared brightness of circumstellar discs at white dwarfs. *Monthly Notices of the RAS*, 449:574–587, May 2015. http://adsabs.harvard.edu/abs/2015MNRAS.449..574R.

[98] J. H. Debes, M. Kilic, F. Faedi, E. L. Shkolnik, M. Lopez-Morales, A. J. Weinberger, C. Slesnick, and R. G. West. Detection of Weak Circumstellar Gas around the DAZ White Dwarf WD 1124-293: Evidence for the Accretion of Multiple Asteroids. *Astrophysical Journal*, 754:59, July 2012. http://adsabs.harvard.edu/abs/2012ApJ...754...59D.

[99] A. J. Mustill, D. Veras, and E. Villaver. Long-term evolution of three-planet systems to the post-main sequence and beyond. *Monthly Notices of the RAS*, 437:1404–1419, January 2014.

[100] C. Berg, G. Wegner, C. B. Foltz, F. H. Chaffee, Jr., and P. C. Hewett. Spectroscopy and spectral types for 387 stellar objects from the large, bright QSO survey. *Astrophysical Journal Supplement Series*, 78:409–421, February 1992. http://adsabs.harvard.edu/abs/1992ApJS...78..409B.

[101] B. Croll, P. A. Dalba, A. Vanderburg, J. Eastman, S. Rappaport, J. DeVore, A. Bieryla, P. S. Muirhead, E. Han, D. W. Latham, T. G. Beatty, R. A. Wittenmyer, J. T. Wright, J. A. Johnson, and N. McCrady. Multiwavelength Transit Observations of the Candidate Disintegrating Planetesimals Orbiting WD 1145+017. *ArXiv e-prints*, October 2015. http://adsabs.harvard.edu/abs/2015arXiv151006434C.

[102] S. Rappaport, B. L. Gary, T. Kaye, A. Vanderburg, B. Croll, P. Benni, and J. Foote. Drifting Asteroid Fragments Around WD 1145+017. *ArXiv e-prints*, February 2016. http://adsabs.harvard.edu/abs/2016arXiv160200740R.

[103] R. Alonso, S. Rappaport, H. J. Deeg, and E. Palle. Grey Dust Transits of WD 1145+017 Over the Visible Band. *ArXiv e-prints*, March 2016. http://adsabs.harvard.edu/abs/2016arXiv160308823A.

[104] J. E. Chambers. A hybrid symplectic integrator that permits close encounters between massive bodies. *Monthly Notices of the RAS*, 304:793–799, April 1999. http://adsabs.harvard.edu/abs/1999MNRAS.304..793C.

[105] M. Jurić and S. Tremaine. Dynamical Origin of Extrasolar Planet Eccentricity Distribution. *Astrophysical Journal*, 686:603–620, October 2008. http://adsabs.harvard.edu/abs/2008ApJ...686..603J.